Traversing Probe Assembly

A Senior Project

presented to

the Faculty of the Mechanical Engineering Department

California Polytechnic State University, San Luis Obispo

In Partial Fulfillment

of the Requirements for the Degree

Bachelor of Science

by

Josh Bugni

Andrew Sofranko

June, 2010

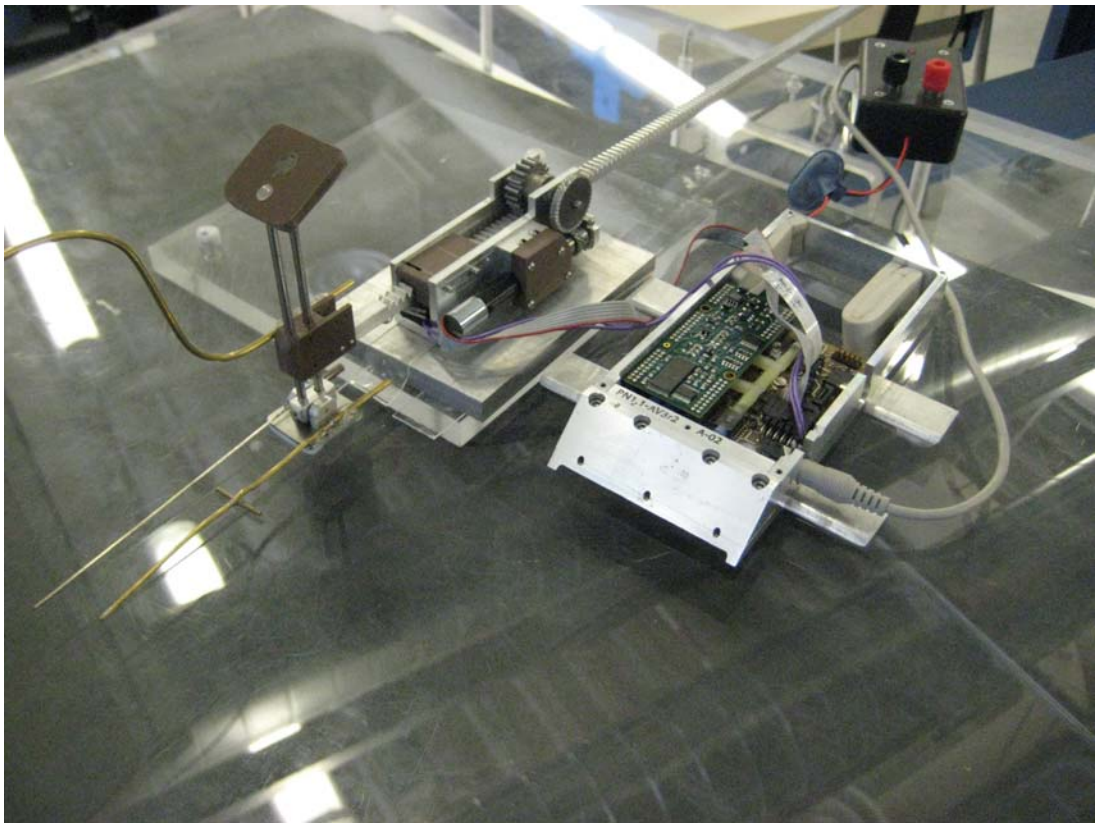

TRAVERSING PROBE ASSEMBLY

SPRING 2010 FINAL REPORT

JOSH BUNGI

ANDREW SOFRANKO

ME 430

Friday, June 5, 2010

Table of Contents

Introduction

On the 29th of September, Josh Bugni and Andrew Sofranko accepted the senior project with Dr. Westphal along with Northrop Grumman to design a traversing mechanism for a Preston Tube/Static Probe assembly. Skin friction measurements are measured on current wings to improve the flight efficiency for tomorrow. Testing at Northrop Grumman has moved from the wind tunnel to in flight testing. Static devices that only sample single locations are the only accurate type of testing available at this point. It is our goal to provide an autonomous mechanism attachable to an aircraft that traverses a group of pressure probes (Preston Tube, Static Probe, Free Stream Probe) to provide the means to better measure skin friction data during flight.

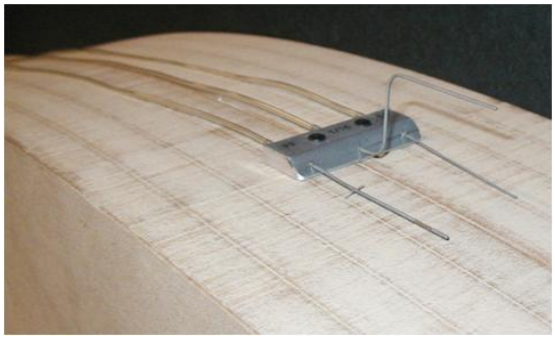

Figure 1.1 Preston Tube/Static Probe/Pitot Tube Assembly

Background

The current goal of collecting skin friction data is to reveal the locations where the transition between laminar and turbulent air flow occurs. This has been done in the past using infrared sensors but the results from the data are unreliable. The few existing devices that measure skin friction during flight are static assemblies. They must be mounted to the aircraft surface, flown, and remounted to a new location if another data point is desired. This takes additional time, extra funding, and cannot collect the data in the exact same conditions. Using static devices requires multiple flights in conjecture with a trial and error process to find the transition zones. A traversing probe assembly will yield the data of multiple test flights under the same conditions.

The device that we will be interfacing with has been used for the past five years to statically measure the local skin friction on the wings of several aircraft. This device houses three probes, a static port and two absolute ports. The free stream Pitot-static tube is positioned above the boundary layer in order to measure the free stream velocity. The static probe and the Preston tube are located against the wing surface and have been used with a vertical stage option to traverse vertically through the boundary layer. The electronics of this device are all contained in an aluminum frame housing with the probes mounted in front. The electronics allow for two 5 pin ports that run on 200 milliamps and a full battery voltage of 11 to 12 volts, typical battery voltage of 7 to 8 volts and will not run below 5.5 volts. There are additionally 2 ports that run on a low current of 50 milliamps and 5 volts. There are three analog input ports that input from 0 to 5 volts.

This device has been mounted to the wing of the aircraft using structural adhesive tape from 3M®. When the device has been attached using the tape, it then needs to be cured for 24 hours at a pressure of 15 psi. To implement this cure, a cover is placed over the entire device, suction cupped down and pressurized to 15 psi. Since the aircraft is not available for such long periods of time for curing, a 20 min cure is implemented instead which results in approximately 50% strength equivalence to the 24 hour cure. The 3M® Company rates this tape at a 4 psi load in shear that won't fail for 10,000 minutes. This gives a 2 psi rating for the 20 minute cure. An additional mechanical safety of factor of 3 is applied giving a final result of 2/3 psi; in other words, for every 2 pounds of shear we will need 3 square inches of the structural adhesive tape.

Since skin friction accounts for half of the total drag on an aircraft it is important to understand the nature of skin friction as it varies over the chord of the wing. The test data for in flight skin friction conditions is limited to static probes that give only one measured location per flight. The reason we need to collect data for skin friction over a larger range of data points can be shown starting with the definition of skin friction, seen in equation (1), in Appendix A. Skin friction depends on the shear stress, free stream velocity and the Reynolds number. Since the Reynolds number, equation (4), is different at each location the local skin friction will vary along the chord of the surface, i.e. the only variable that is changing is position. To find the total skin friction the shear stress must be integrated along

the entire surface, equation (3). The only term that depends on position is x so we can rearrange the integral so the x term is the only one left inside the integral, equation (6). This makes it easy to see that the skin friction is going to depend on the inverse of the fifth root of x. With a location close to the leading edge, i.e. a small value of x, there will be higher local skin friction then a location further down. This tells us that there is a higher effect of friction at the leading edge and will decrease non-linearly as position moves away from the leading edge. This function is difficult to model using a mathematical approach for complex geometries such as the swept wing of the White Night and thus test data must be used for real world analysis. The skin friction will be greater for turbulent section when compared to laminar sections. This is due in part to the mixed energy in the turbulent section which provides a larger component of air velocity at the surface, resulting in high shear stresses and ultimately larger friction force. This will allow us to locate the transition zone with skin friction measurements because the laminar section will generally have less friction then turbulent, noting that the location in the x direction will have the opposite effect.

Objectives

Design Requirements

The overall objectives for the traversing probe mechanism are listed below. They were found as a result of reviewing the requirements and specifications from our sponsor. They state the criteria for which the completed product will be measured against.

- Provide a mechanical system capable of traversing multiple probes along an aircraft's surface during flight.
- Static and Preston Probe tips must remain in contact with the surface.
- The system must be autonomous and compatible with the existing Boundary Layer Data System Interface.
- The system must be light enough to be attached with adhesive tape and robust enough to withstand the environmental elements of flight.

Design Specifications

The table below lists the design specifications for our project. These specifications were derived from project objectives and goals. The table lists the parameters along with how hard they will be to achieve (risk factor). Weight is our number one concern in the design specifications. The product must not exceed 1 pound due to the adhesive tape needed to attach the assembly and the safety regulations required by the Federal Aviation Administration.

Table 1.1 Design Specifications with Legend

Parameter Description	Target Requirements	Risk	Compliance
Weight	< 1 lb	H	T
Travel Length	500 mm	M	T
Height	<70 mm	L	T
Width	100 mm	L	T
Traversing Speed	>2 mm/s	M	T
Air Speed	400 ft/sec (max)	H	T
Wind Loads	150 psf	H	T
Temperature	-60°C to +40°C	H	A, T
Positioning Accuracy	± 1 mm	H	T
Probes touch along mildly curved surface	Must	L	I
Interface Compatibility	Must	L	T
Aircraft Maneuvering	<3Gs, 2G normally	L	T, A
Adhesive Structural Tape	$2in^2$ per 3lb of shear load	M	I
Control	Autonomous	M	I
Aircraft Vibration Loads	2 – 3 Gs	M	T, A
Allowable misalignment along Wingspan	Small to none	M	T

Legend	
Risk	Compliance
Low (L)	Analysis (A)
Medium (M)	Test (T)
High (H)	Inspection (I)

Design Development

Drive System Concepts

To come up with the best design, we first had to start with a list of concepts. Selecting the final concept was done by using a decision matrix. Our decision matrix compares our top selected concepts to design criteria using a four point scale. The selected criteria are then weighted using a 5 point scale. The weight and size were our top concerns when selecting our concepts. Of our 8 concepts we estimated that the hollow tube and the rack & pinion were the best choices. Our final decision was made between the two by stating which one we had the most confidence in. We believe that the Rack and Pinion Drive system will operate the best under the flight conditions and is capable of being constructed with a minimal weight and profile.

Table 1.2 Drive System Decision Matrix

Concept Criteria	**Points**	**Hollow Tube Friction Drive**	**Telescoping Antenna**	**Rack & Pinion Drive**	**Crank Drive**	**Joint Armature**	**4 Bar Linkage**	**Track Guided Drive**	**Lead Screw**
Weight	5	4	3	4	2	2	2	1	2
Size/Shape	5	3	4	3	1	1	1	1	3
Confidence	4	2	1	4	1	1	1	1	1
Construction	4	3	1	3	3	1	3	1	3
Cost	3	2	3	2	4	3	4	1	2
Temperature	3	3	4	4	4	4	4	3	3
Probe Attachment	3	4	4	4	4	4	4	2	1
Plumbing	1	4	4	2	2	2	2	2	1
Weighted Total		86	80	95	69	58	69	38	60

Rack and Pinion

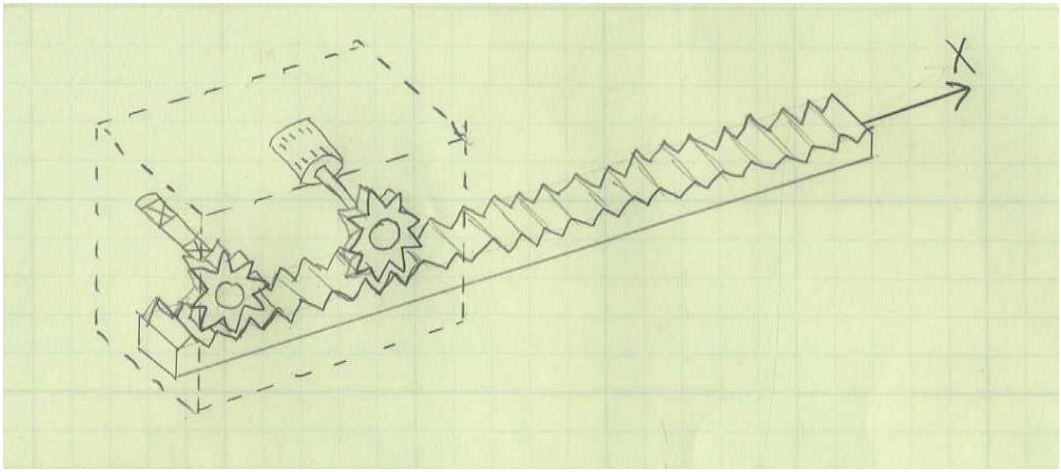

Figure 1.2 Rack and Pinion

In this concept, the probes will be attached to one end of the rack gear and the extension of the rack will provide the traversing length. The pinion gear and motor will be enclosed in a housing that will attach to the wing with the structural adhesive tape. When the probes are at full back position, the rack will extend past the back of the drive housing.

Hollow Tube Friction Drive

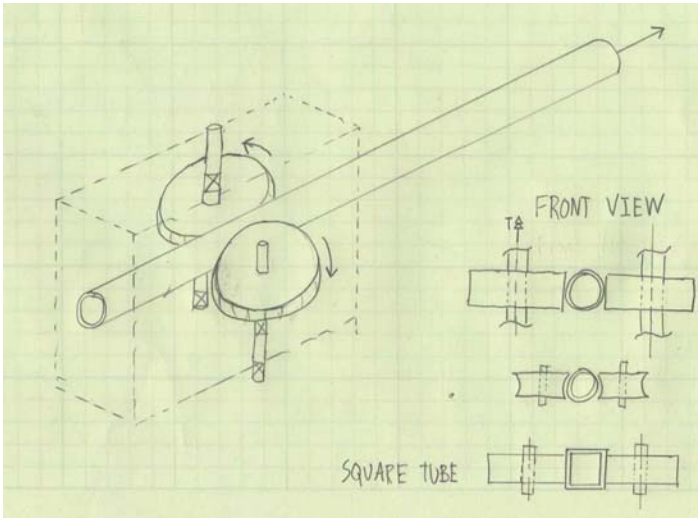

Figure 1.3 Hollow Tube Friction Drive

For this concept, the probes will be attached at the end of the tube and the plumbing for the probes will be enclosed in the tube. Two wheels squeeze the tube and drive the tube with friction to provide the traversing distance. The wheels and motor will be enclosed in a housing that attaches to the wing.

Lead Screw

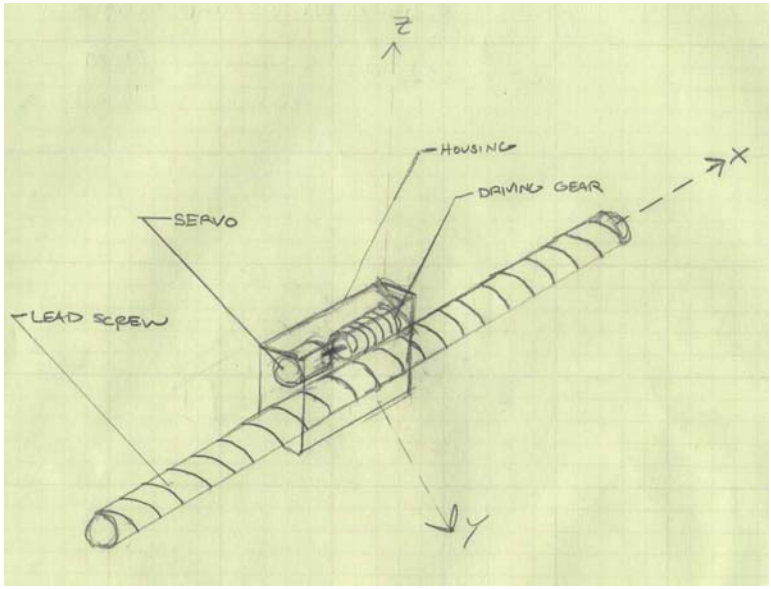

Figure 1.4 Lead Screw

The probes will be attached to a mounting piece that is attached to the end of the lead screw. This mounting piece will prevent the probes from rotating as the lead screw rotates. The motor and the lead screw pinion will be enclosed in an aerodynamic housing.

Triangular Scissor Lift

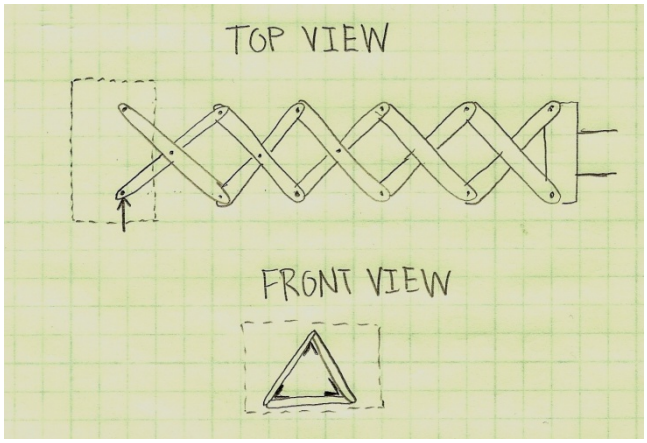

Figure 1.5 Triangular Scissors Lift

With multiple two bar scissor linkages, a large distance can be traversed with a small amount of actuation. By arranging three of these scissor lifts into a triangular set up, more rigidity would be achieved. The frontal area of this device is rather large. This concept is limited in its ability to traverse against curved surfaces.

Crank Arm

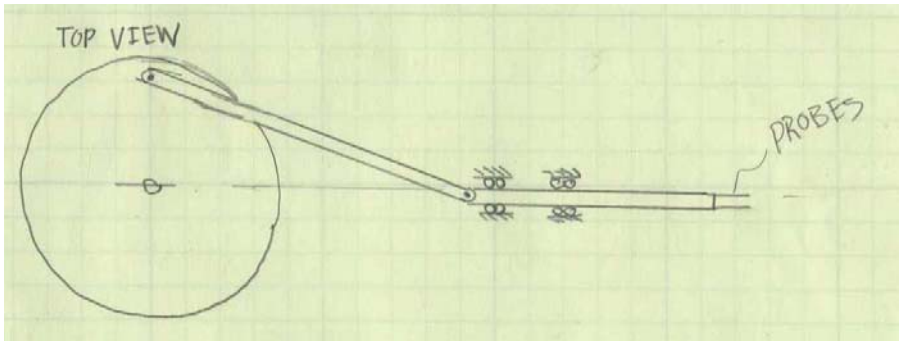

Figure 1.6 Crank Drive

This concept utilizes a motor which will drive a crank arm wheel and transfer the circular motion to horizontal motion. This will require multiple mounting locations as the horizontal motion bar needs to be restricted by guides. This concept requires a large horizontal profile and multiple mounting points.

Joint Armature

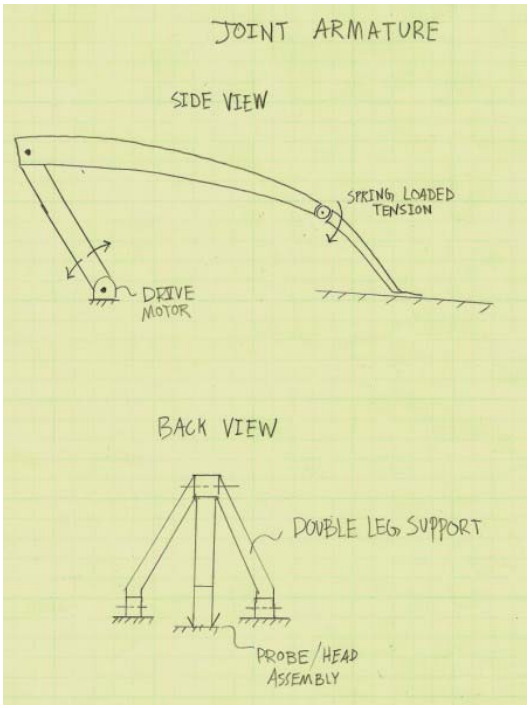

Figure 1.7 Joint Armature

With a pivot point at the back end being driven by a motor, a 'parallel' bar will reach up and over to provide the traversing distance. By adding a joint out at the tip and loading it with a spring, the probes can be kept pressed against the surface. Two legs will be needed for stability. The large frontal area exposed to drag will require a larger torque from the motor to overcome the drag force as well as more structural adhesive tape to keep the set up mounted.

Telescoping Antenna

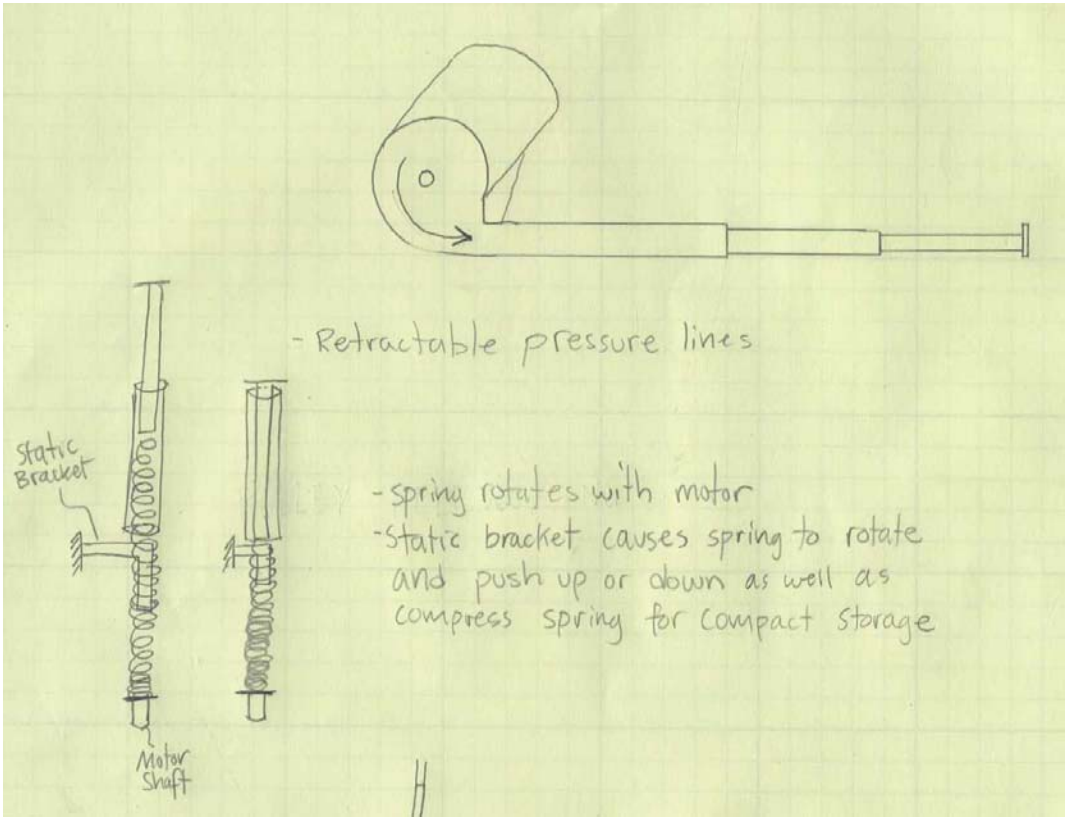

Figure 1.8 Telescoping Antenna

This telescoping concept is similar to a car's automatic radio antenna device. Most of the old automatic car antennas use a rack and pinion set up, which would be included in our rack and pinion concept. The newer version of these automatic antenna devices use a spring that allows it to be compact. A spring is attached to the rotating motor shaft. By placing a static bracket down the center of the spring, the rotation of the motor will cause the spring to screw upward from the bracket. As the spring rotates and pushed outward, it pushes the antenna out and as the spring rotates and screws back past the bracket, it will compress into convenient storage. When the antenna is extended, it can be pressed inward with little force due to the spring's compression, making this concept inadequate for our needs.

Track Guided Stationary Lead Screw

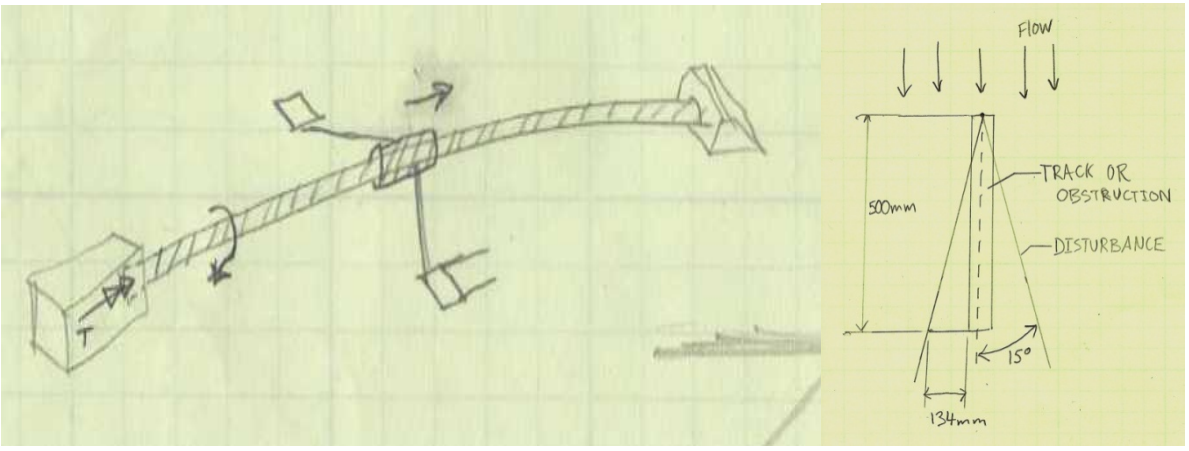

Figure 1.9 Track Guided Stationary Lead Screw with Line of Disturbance

A lead screw is mounted at both ends to keep it stationary in the lateral direction but is still able to rotate freely. By driving with a motor from the back end, a sleeve on the lead screw will move back and forth so long as the sleeve is not allowed to rotate. To keep it from rotating, two arms will stick out perpendicular to the lead screw and press against the wing surface. By loading these arms up with a spring, they will always press against the wing In order to not disturb the flow that we are analyzing, the distance perpendicular to the lead screw will need to be calculated. For a general case, 15 degrees of disturbance will be created. With a travel of 500 mm, the arm will need to reach 134 mm to the side, which is with no factor of safety. The probes can be mounted on the end of these arms to reach out of the disturbed flow.

Surface Contact Concepts

A design matrix was also made for the surface contact concepts. This matrix was done on a five point scale and revealed that the Spring Loaded System was superior when compared to the other concepts on weight, cost, profile, ease of construction, and reliability. We originally were considering implementing both the Internal Spring Loaded System and the Spring Loaded Joint but after further review found the Internal Spring System to cause problems and impede the movement of the arm. Using a single Spring Loaded Joint with a modified second pivot arm and foot will be sufficient for keeping the probes in constant surface contact.

Table 1.2 Surface Contact Decision Matrix

Criteria	Weight	Internal Spring Loaded	Aero Fin	Spring Loaded Joint	Catheter	External Spring System
Weight	4	5	5	4	3	5
Cost	2	4	4	4	2	4
Profile	3	5	1	4	4	1
Construction	3	1	4	3	2	3
Reliability	2	2	3	2	2	2
Weighted Total		50	49	49	38	44

*note – We originally selected a spring loaded design based on estimated criteria and found later after testing that the spring designs gave us issues and the aero fin was later implemented for the final design and gave us much better results.

Internally Spring Loaded

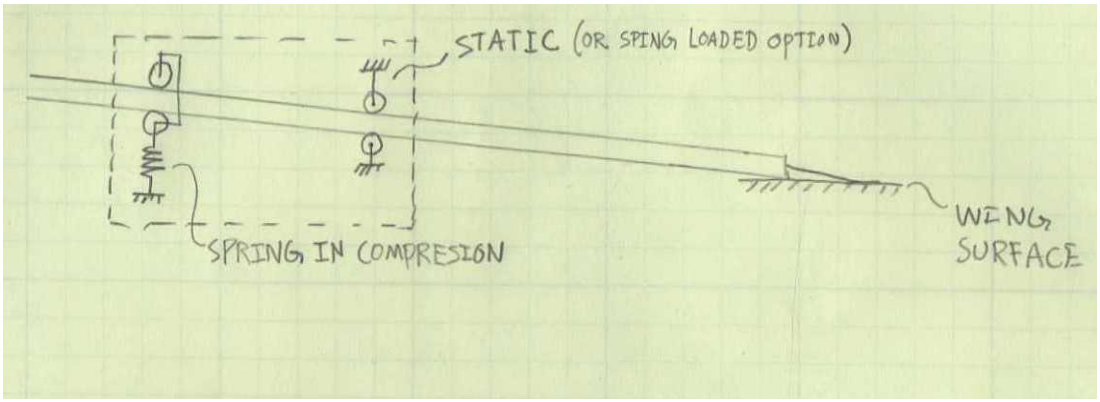

Figure 1.10 Internally Spring Loaded System

Inside of the motor housing, a spring will push up against the arm in the back. A pivot will be at the front of the housing in order to minimize the hole that the arm will protrude out of. As the arm extends out of the housing, the spring will hold the arm against the wing surface.

Externally Spring Loaded

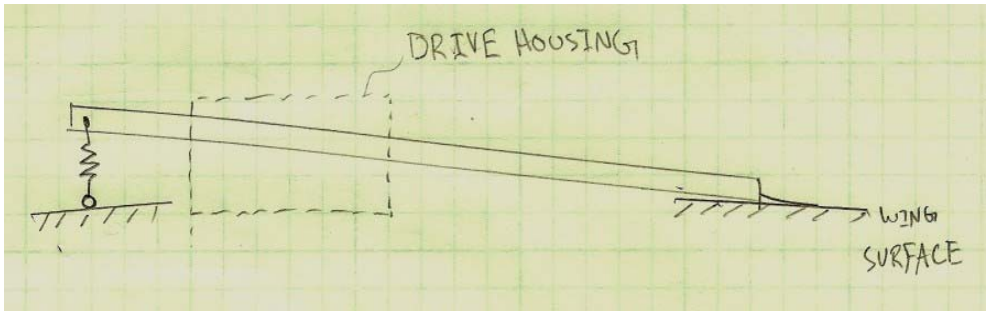

Figure 1.11 Externally Spring Loaded System

At the very back end of the arm a spring set up will push up against the arm. A pivot point in the drive housing will cause the spring to push the tip against the wing surface. By having the spring further back compared to the internally loaded spring, there will be more distance for the spring to stretch and compress.

Aero Fin

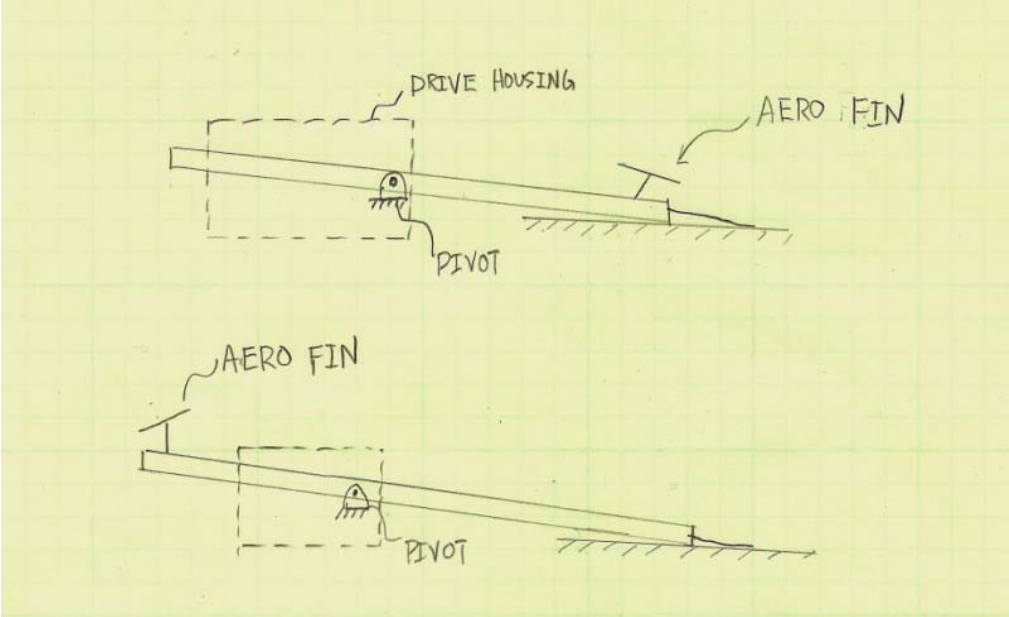

Figure 1.12 Aero Fin

By mounting a fin at the front of the driving arm, the air stream will provide the force that will press the probes against the surface of the wing. The fin could also be inverted and located at the back end of the arm.

Catheter

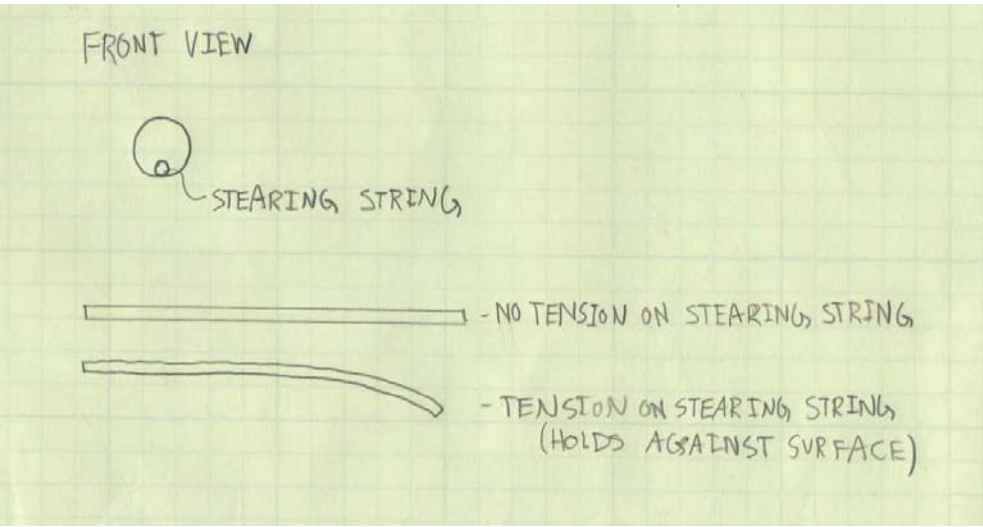

Figure 1.13 Catheter

Similar to the steering of a catheter in medical applications, the arm with the probes attached at the front would consist of a tubular structure with a steering string located on the bottom against the wall of the tube. By pulling on the steering string, the tube will flex and push against the surface of the wing.

Spring Loaded Joint

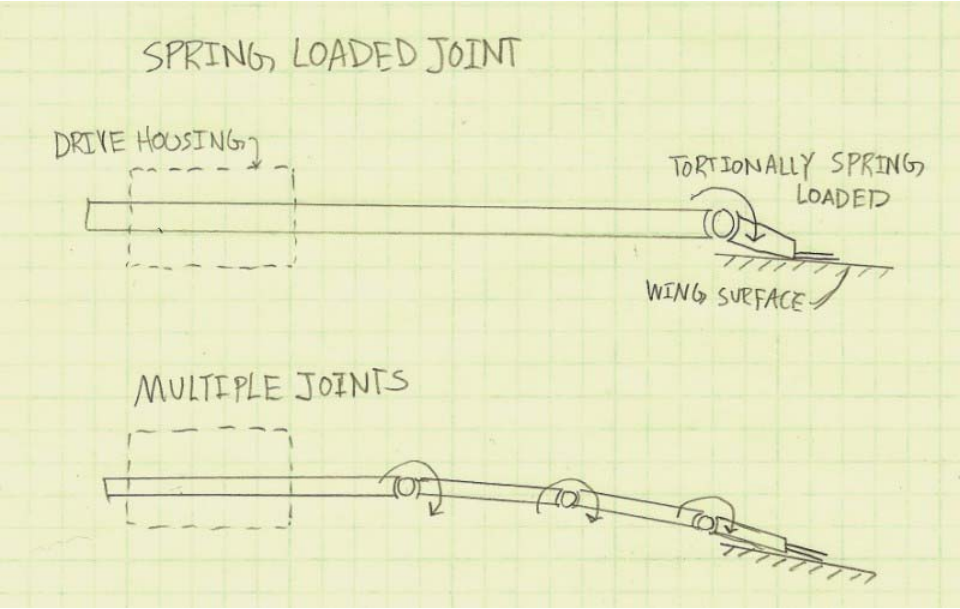

Figure 1.14 Spring Loaded Joint

Towards the front of the drive arm a joint will be spring loaded so that the tip where the probes are located can be pressed against the surface. Multiple joints could be considered but would complicate the drive system if a joint must past through the drive housing.

Location Sensor Concepts

Knowing the position of the probe is a critical objective in our project. We will select a sensor that will track the traversing distance of the probe. The three location sensors considered were a Magnetic Integral Encoder, an Optical Encoder, and a String Potentiometer. The selection of sensor was dependent on the drive system. After selecting the rack and pinion drive system, the most compatible and logical choice that will give us an accurate location of the probe relative to its starting location is the Magnetic Encoder. A decision matrix shown in Table 1.3 shows how the three sensors scored in comparison to each other. We found that the Optical Encoder would contribute the least weight to our system but we had more confidence in the Magnetic Encoder. The Magnetic Encoder will attached to our motor and be a more reliable measurement device.

Table 1.3 Location Sensor Decision Matrix

Criteria	Weight	Magnetic Integral Encoder	Optical Encoder	String Pot
Weight	4	3	4	1
Cost	2	3	3	3
Reliability	3	1	4	2
Compatibility	3	3	4	1
Weighted Total		34	42	19

Description of Final Design Before Build

Before we drew up the selected concepts in Solid Works, we molded the system using particle board and screws to better understand the geometry that we were dealing with. Pictures of this model can be seen in Appendix C. Once we had an idea for the size that the components would need to be, we modeled our system in Solid Works.

The figures below show the assembly of our selected concepts. The rack will be driven by a dc motor coupled with a gearhead. The probes will remain in contact to the surface using a spring located at the front of the arm that attaches to the probe foot assembly. The position will be monitored using an integrated optical encoder attached to the motor. A fairing will act as insulation to protect the internal mechanisms from the cold environment as well as provide an aerodynamically streamlined shape to minimize drag.

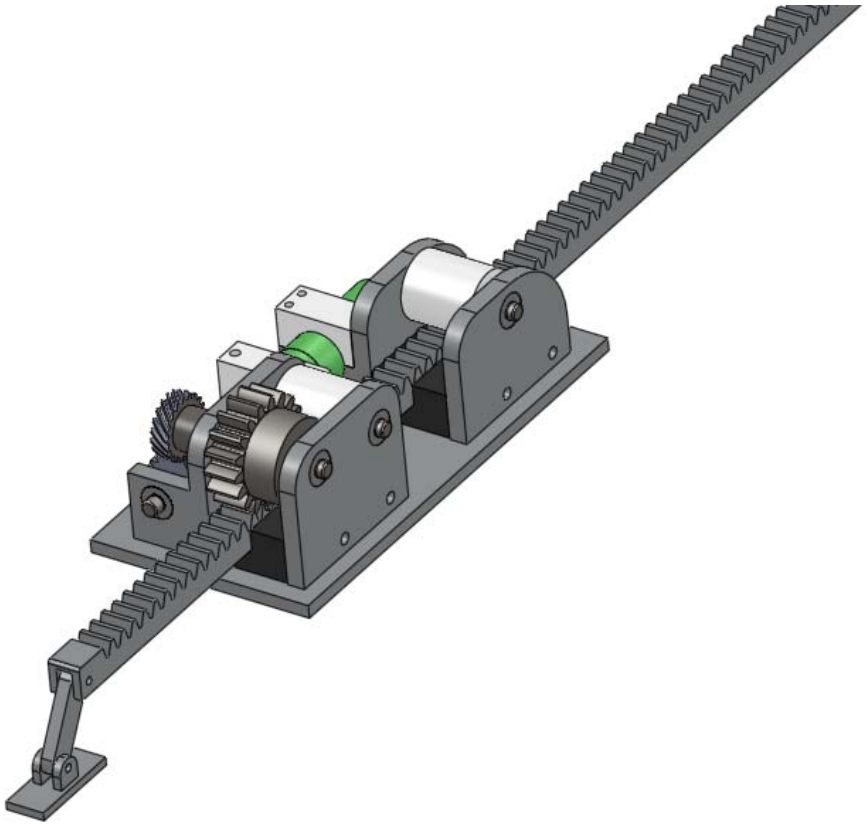

Figure 2.1 Final Design before Build, January 1st, (shown without housing)

When we had a solid works model, we decided to build our system in a rapid prototyping machine. This was a useful exercise because we needed to make sure that the rack that we were going to manufacture ourselves would have the correct geometry to interface with the chosen pinion gear. Geometry for the motor and helical gears was also validated with this prototype. Pictures of the rapid prototyped model can be seen in Appendix D.

Analysis

Tape Mounting Considerations

The amount of tape required to attach the probe assembly is a function of the estimated wind and 3G loads. With a conservative value of 200 pounds per square foot of pressure incident on the frontal and side areas of the assembly, we estimate that it will require 5 square inches of tape. This is an acceptable amount for our final design and can be easily integrated with the use of attachable feet. The addition of feet has been used for the previous static probe assemblies and has proven to work well. See Appendix F for the full calculations. With a tape area of 5 square inches, we will have a safety factor of 1.5 with the conservative 200 psf load analysis.

Probe Position

The position of the probes is deciphered with the encoder. The encoder has 10 counts per revolution and with our 1:128 gear ratio and the 0.75 diameter of the pinion, there will be approximately 33,000 counts for half a meter traversing length. Each millimeter is equal to approximately 60 counts. The system will not know where it is on start up so it will move to a limit switch and zero its position and move from there. The position of the probe tips, i.e. data points, will be measured relative to the front of the base depending on the amount of encoder ticks that the motor has rotated through and correlated to the actual position. This will be calculated in the program in the BLDS board. Speed and position calculations can be seen in Appendix F.

Deflection of Rack

At maximum extension and maximum yaw loads the rack will be in its worst case scenario for deflection. Analysis has shown that deflection for this scenario will be under an inch. Analyzing the first natural frequency of the rack shows that it would take a very high frequency to cause resonance. Further testing at speed greater than our wind tunnel can produce will be needed to insure the system is not unstable at the frequencies and amplitudes of our design conditions.

Drag Force on Frontal Projected Area (Motor Stall Torque)

After the final design was built, the frontal area of the probe foot assembly attached at the tip of the rack was analyzed for an equivalent torque seen by the motor. With our design, we have a frontal projected area of 1.825 in^2 which correlates to a torque at the motor of 0.63 mNm. The stall torque of the motor is 2.89 mNm which gives us a factor of safety of 3.5. At idle conditions, for data acquisition, the force incident on the rack directly is 2.5 pounds for the conservative 200 psf value. Our testing showed the stiction in the system to be around 0.5 pounds indicating that the stiction will be overcome at maximum conditions and additional breaking will be needed. The current H bridge drive system that the BLDS board uses does not allow for motor breaking so we recommend either providing an additional breaking system or redesign of the board to incorporate motor breaking.

Figure 2.2 Frontal Projected Area

Probe Speed for Motor Selection

We used the desired probe speed to select a proper motor and verified that the torque of the chosen motor would overcome the aerodynamic loads caused by the foot assembly. We selected a motor currently being used by the stage BLDS assembly. This allowed us to use current motors already purchased for testing our device. See Appendix F for hand calculations.

Force Analysis for Angled Fin

When the foot design changed from the spring design to the angled fin, we needed to consider the additional horizontal force that would be seen by the motor as a torque. We also needed to make sure the fin provided enough vertical force to keep the probes in contact with the surface. See Appendix F for hand calculations.

Temperature

Our main concern with the minimum temperature is that some moving components require certain tolerances for operation. When the minimum temperature range is reached, the components will shrink at different rates due to different material and must have a certain amount of slop designed into them so when the minimum temperature is reached, the geometry does cause binding.

- The rack alignment sleeves will sufficiently work under the minimum temperature with an additional 0.002 inches of clearance.
- The foot assembly linear bearings need to have a clearance of 0.0007 inches.
- All the parts have specifications that will meet the minimum and maximum temperature conditions.

Safety

ASME's first fundamental cannon states that engineers should hold paramount the safety, health, and welfare of the public in the performance of their professional duties. Our project's safety is considered in the weight requirement. This device is attached with

adhesive tape and must not exceed the weight requirement. Worst case scenario is that the device comes loose during flight and separates from the aircraft. FAA laws state that any objects that fall off an aircraft over 1 lb is a catastrophic failure. Any objects weighing less than 1 lb are considered a marginal issue and occurs rather often. Northrop Grumman has designated our weight requirement in preparation of adhesive attachment failure by setting our weight requirement to half the FAA threshold. In addition to this safety consideration, we designed into our attachment system a 1.5 factor of safety to insure that our assembly will not become unattached from the aircraft.

Manufacturing

Rack Construction

Since our most concerning design requirement is weight, a steel rack is not applicable. With the rack protruding out a large distance, vibration is a concern so a stiff material is desirable, making plastic materials not applicable. Another concern is the temperature range with the minimum being -60 degrees Celsius, a material that becomes brittle at these temperatures is not applicable. The most suitable material to use is aluminum. This posed a problem because no supplier had off the shelf racks made out of aluminum so we chose to construct a rack ourselves.

An ideal gear is made with a special cutting tool on vertical axis mill but since we do not require extreme accuracy that is usually associated with ideal gear design, we have come up with a simple process to construct our rack. We only need a simple v shaped tooth at a pressure angle of 20 degrees to match up with the pinion gear. This means that we need an angle of 40 degrees between the teeth faces so we can achieve this feature with a 40 degree chamfer tool and cut the v shaped channel in a couple passes in a CNC mill.

We ran into an issue with the shape of the rack teeth in one small portion. When the 25 in long bar stock was chucked up into the CNC mill, three chucks were used. One of the gaps between the chucks was wider than the other and with the path of the tool approaching from only one side, rather than from both sides, the bar stock flexed as it made it path. This

created a twist in the small section where the gap was large. The effect was as this portion passed through the sleeves, the rack rotates axially and thus lifts one side of the foot assembly off the surface and ultimately lifts the probe off the surface. The solution to this problem is simple, the chucks should be spaced evenly apart, a minimum gap size should be used, and the tool path should approach the rack from both sides to even out any twisting. The suggested tool path can be seen in figure 3.1. It is crucial that raw material used for the rack to be straight. We ordered our piece at a quarter inch and cut the teeth from that piece. It would improve the motion of the probes if a larger stock piece was ordered and milled down the quarter inch size to insure straightness.

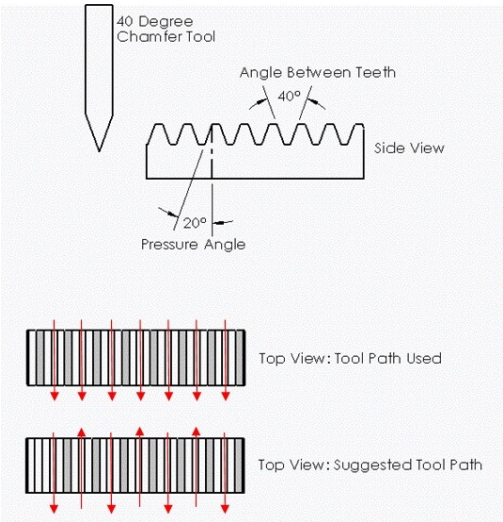

Figure 3.1 – Rack Construction- Suggested Tool Path

Helical Gears

The frontal projected area needed to be minimized to decrease the drag force. If the motor were to be attached directly to the pinion that drives the rack, the motor would be oriented perpendicular to the air flow and would cause a large frontal area. We chose to use helical gears so that the motor can be reorient by 90 degrees and thus parallel to the flow.

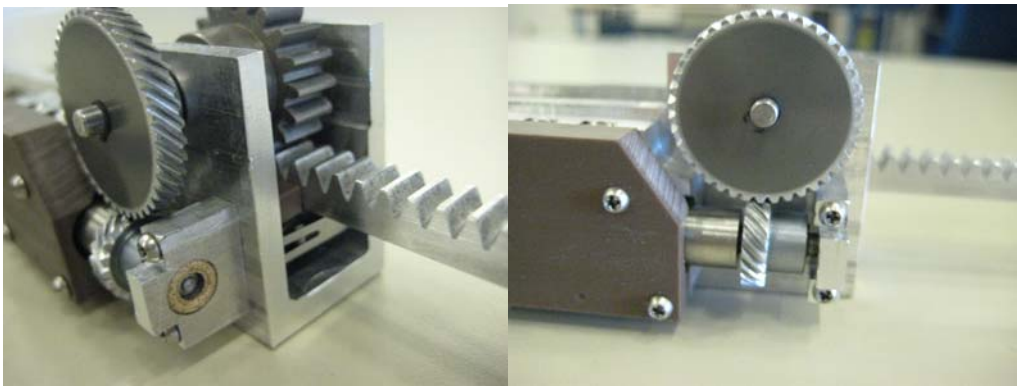

Figure 3.2 – Close up Picture of the Helical Gears

After we constructed our first iteration, we found that the foot assembly was difficult to construct to fit under the clearance associated with the two 20 tooth helical gears, between the bottom of the base and the bottom of the rack. By increasing the teeth of one of the gears to 40, the clearance was increased enough to fit the foot assembly between the bottom of the base and the bottom of the rack as illustrated in figure 3.3.

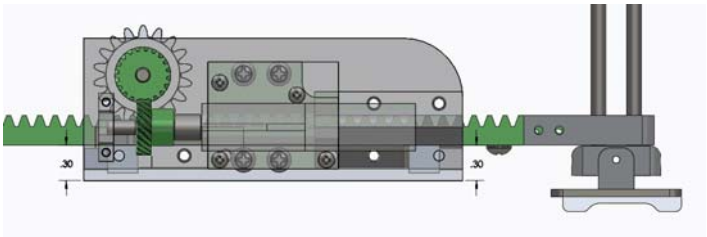

Iteration II

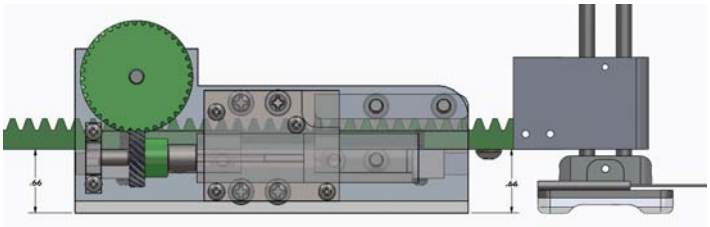

Iteration III

Figure 3.3 – Clearance issues with different size helical gears.

Also, by increasing the second helical gear, the speed will be decreased by a factor of two, ultimately changing the gear ratio from 64:1 to 128:1 giving us a more ideal speed. This will also decrease the torque seen by the motor that is caused by wind loads which will give us a higher factor of safety for stalling the motor and will decrease the amount of power consumed.

Motor Mount

The MicroMo motors provided to us have no screw-hole attachments so we chose a clamp method. Two half cylinders the size of the motor clamp the motor in place using one side as aluminum and the other side as Delrin. This provided us with sufficient alignment of the motor output shaft without the need for a coupling to the first helical gear.

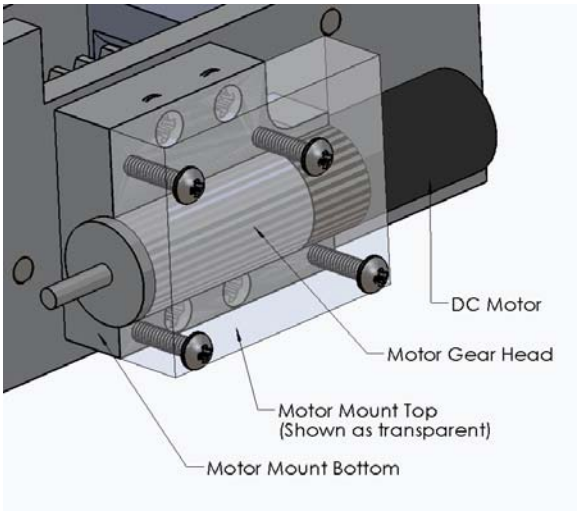

Figure 3.4 – Motor Mount

Foot Design Assembly

After we had completed our Final Design before Build, we planned on using a single armature that uses a torsion spring to hold the probe foot to the surface. The problem with this design is that the position of the probes will vary depending on the curvature of the surface, giving rise to an unknown error depending on the curvature of the surface; error depicted in figure 3.5. Our interface can only tell the position of the rack tip using the counted encoder ticks. A solution to this error would be to add a potentiometer to measure the angle between the rack and forearm and thus could calculate the actual position of the probe. This would introduce wires in addition to the probe tubing that would need to be routed back to the BLDS interface board. We decided that this design would have undesirable error that would cause more issues with trying to measure the error so we went with an absolute position design with the use of axial motion shafts.

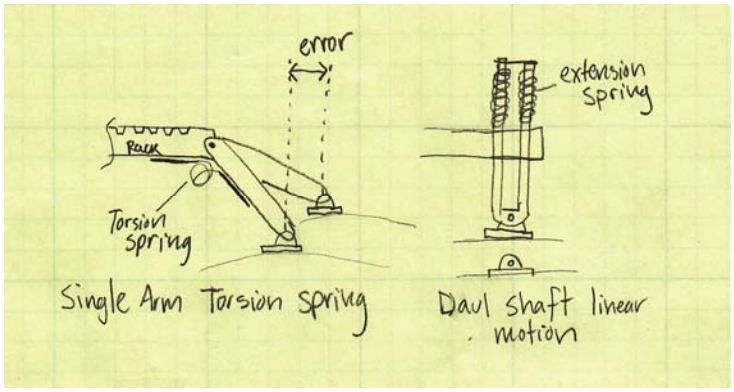

Figure 3.5 – Torsion Spring Error

The next Iteration that we came up with to fix the error associated with the torsion spring design, incorporates the foot being positioned with a vertical shaft that moves linearly. This will allow the probe foot to always be in the same position relative to the rack tip. With only one shaft, the foot would be able to rotate about that shaft and would thus not keep the probes parallel to the flow so a second shaft is needed to keep the orientation stable. To provide a force that keeps the foot pressed against the surface, an extension spring is used. A compression spring would need additional space between the foot assembly and would require raising the rack and ultimately increasing the frontal projected area too much so extension springs are more desirable. The extension spring iteration can be seen in figure 3.6.

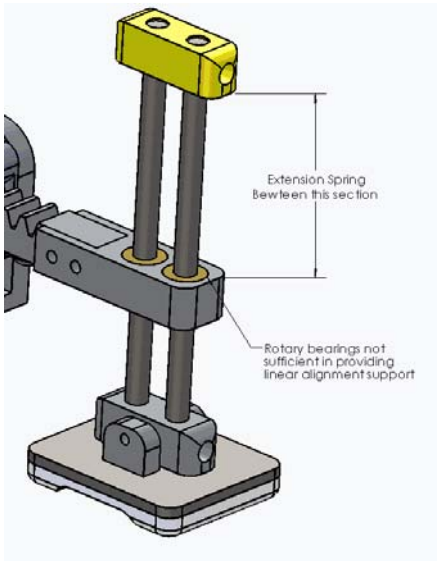

Figure 3.6 – Extension Spring Surface Contact Design

After testing the extension spring design, we found that the system had trouble with binding up. This was due to the fact that the force that was needed to hold the probe foot against the surface that came from the spring had an equal and opposite reaction force seen on the rack. This force on the rack bends the rack upward causing more friction in the sleeve and pinion area which ultimately cause the system to bind up and stop. This led us to a final iteration that provides a force that is not seen by the rack by using an angled aero fin.

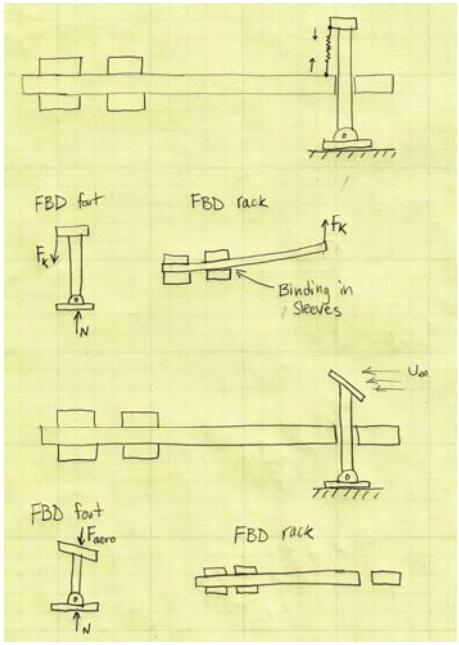

Figure 3.7 – Spring Force FBD's

Our last iteration for the foot assembly uses the momentum change of the airflow by virtue of an inclined fin to provide the force to hold the foot against the surface. This eliminates the reaction force seen by the rack and does not cause the system to bind up. The aerodynamic foot assembly can be seen in figure 3.8. A platform made with Teflon feet and a sheet metal upper surface allows the probes to be attached with silver soldier. A pivot point connects the shafts to this platform so the probes will be tangent to minimal curvatures. A Delrin tip is attached to the end of the rack to provide linear bearing to the shafts to hold them vertical. At the top of the shafts is a sloped piece of Delrin to provide the aerodynamic force.

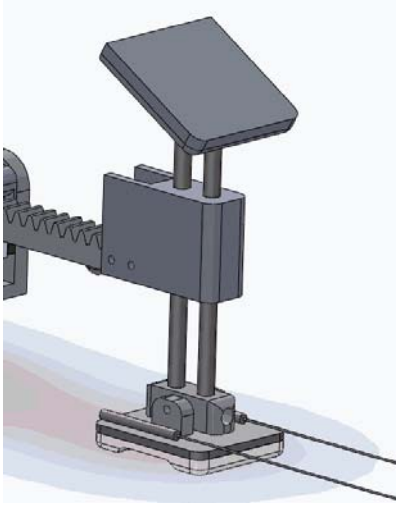

Figure 3.8 – Inclined Fin Assembly

When we first built the rack tip piece, we used the bearings that were purchased for the rotating shafts in the drive system, seen in figure 3.6. We found out that the rotary bearings provided no lateral support since we used only one bearing for each shaft. If a second bearing was used so that each shaft was held by two bearings spaced further apart, there might have been more lateral support; although since the bearings are designed for rotational support only, we decided to construct our own linear support system from Delrin which turned out to be more than sufficient.

Roller & Sleeves

Our first iteration called for rubber rollers to help guide the rack through the pinion and Delrin sleeves. After our first iteration testing, we concluded that the rollers provided too much downward force and hindered the smooth movement of the rack which prevented the motor from moving the rack. We also noticed that just after a few cycles, the aluminum rack was damaging the rubber rollers. After redesign of this system, we used the same style sleeve that holds the sides and bottoms of the rack and proved to be a sufficient downward force to hold the rack in place with enough freedom to move. The special features of this part include a fillet on the edges so the rack teeth do not catch as they slide into the slot.

Two sled style sleeves are mechanically fastened to the aluminum base and provide support for the rack at the desired distance from the Pinion gear. Another big advantage of

the Delrin is its smooth surface, which aids in lubricating the rack as it slides through the assembly. As stated above, we removed the rubber rollers and replaced them with one extra Delrin sled that holds the top of the rack. The rack is now secure and has support from all directions as it passes though the system.

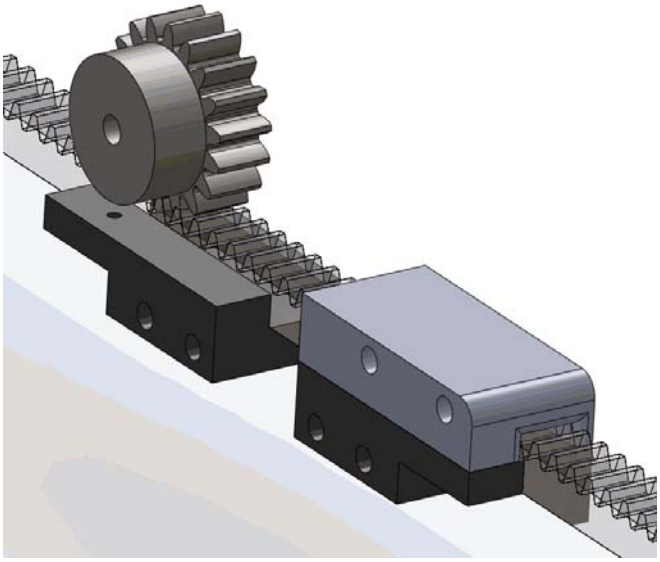

Figure 3.9 –Sleeve/Sled set up for Rack Alignment

Limit Switches

A final iteration was made to the Delrin near the end of our manufacturing process. We removed some material from the bottom of the sled to make room for limit switches. The limit switches will be connected to the motherboard and provide feedback for when the rack reaches its limit. Screw heads act as stops that activates the limit switches and also provide us with a dead stop to prevent the rack from ever falling out of the assembly.

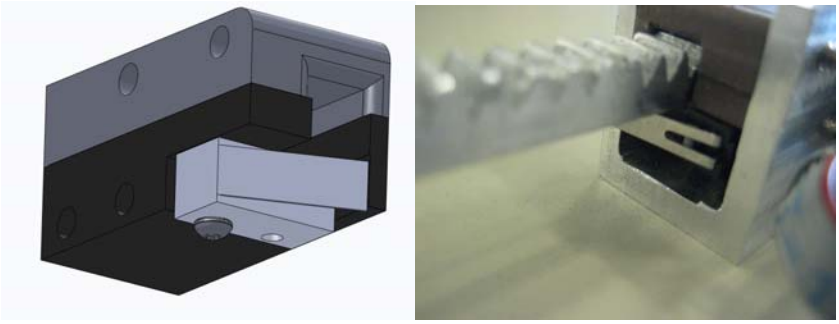

Figure 3.10 – Limit Switch Integrated into Lower Sleeve

Cover/Fairing

In the last couple weeks of our senior project, our design team set out to build a composite fairing for our assembly. The process had been on hold until now due to the unknown amount of revising and iterations the dimensions underwent in our assembly. Now having completed the manufacturing process for our assembly, we knew the size and shape required to fit our project and still be small enough to have a low projection area so that the needed amount of tape would not be excessive. The purpose of the fairing is to protect the inner workings of our assembly from the environment and also decrease the aerodynamic loads.

We sought help from both Dr. Mello (Composites Faculty Advisor) and Dan Davis (Composites Lab Assistant) for this process. Our first step was to construct a tool that would be the mold for our part. We decided to make a rapid prototype of a mold and use that to shape our carbon layup. The properties of the plastic from the rapid prototype are not ideal but allowed us to quickly model the shape we needed. We constructed the shape in Solid Works by taking the inverse shape of our final assembly and rounding the edges. We took the rapid prototyped mold to the composites lab and began the composite process.

The composites material L929 was selected because it is an easy carbon impregnated epoxy that could be heat molded into our tool. We selected 3 layers laid at 0/45/0 degree orientation as to have tensile/compressive strength in all directions. The composite was bagged and a vacuum seal was checked. The bagged part was placed in the ASC autoclathe with a cure recipe of 250 degrees Fahrenheit and no pressure for 3 hours. After the composite had completed the curing process, clearance holes were added to allow the rack to protrude out of the fairing.

The final composite piece did yield during its curing process. It was not a critical yield but enough to cause enough deformation as to not allow us to cover our assembly. The cause of the failure was high temperature melting and yielding of the low density rapid prototype plastic. To ensure that this does not happen again in the future, we recommend a stronger mold material be manufactured to provide more support to the composite material. Using the high density RP machine might be sufficient but metal would be more appropriate. The

completion of this housing is not critical to the completion of this project as we were still able to test in our wind tunnel's maximum wind speeds. If further testing is to be done at the design conditions, a fairing would be critical.

Figure 3.11 - Cover

FINAL DESIGN

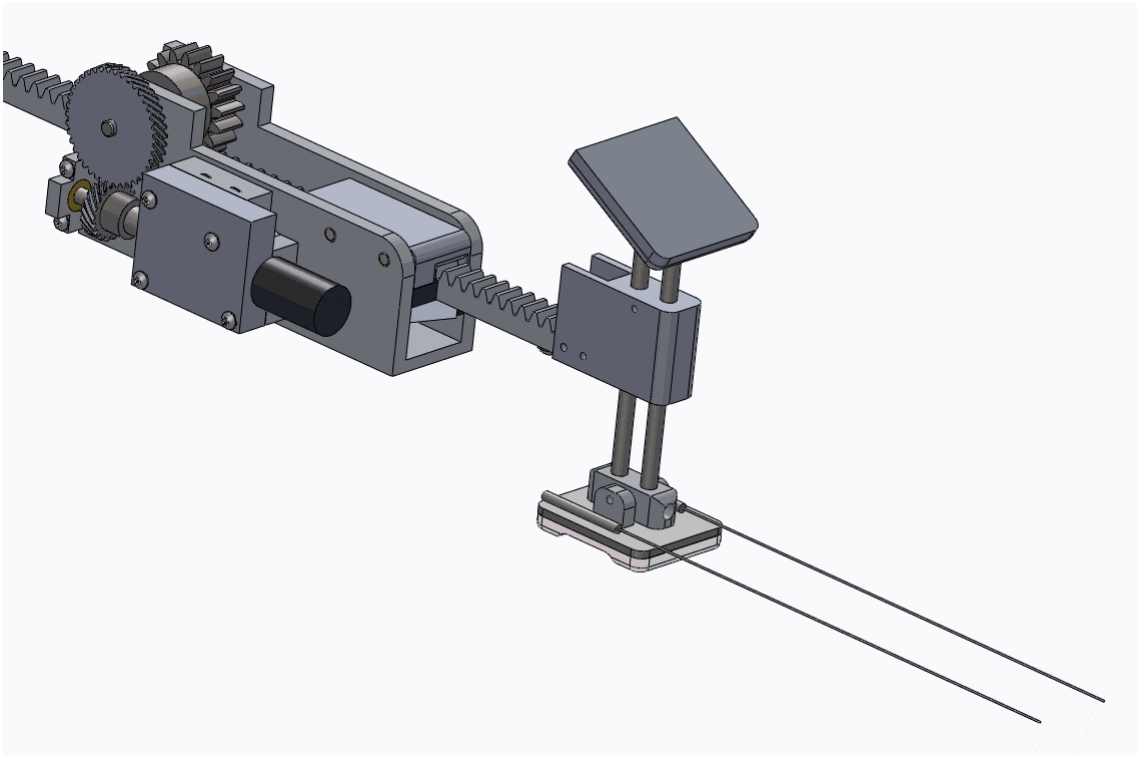

Figure 4.1 - Final Design Solid Works Model

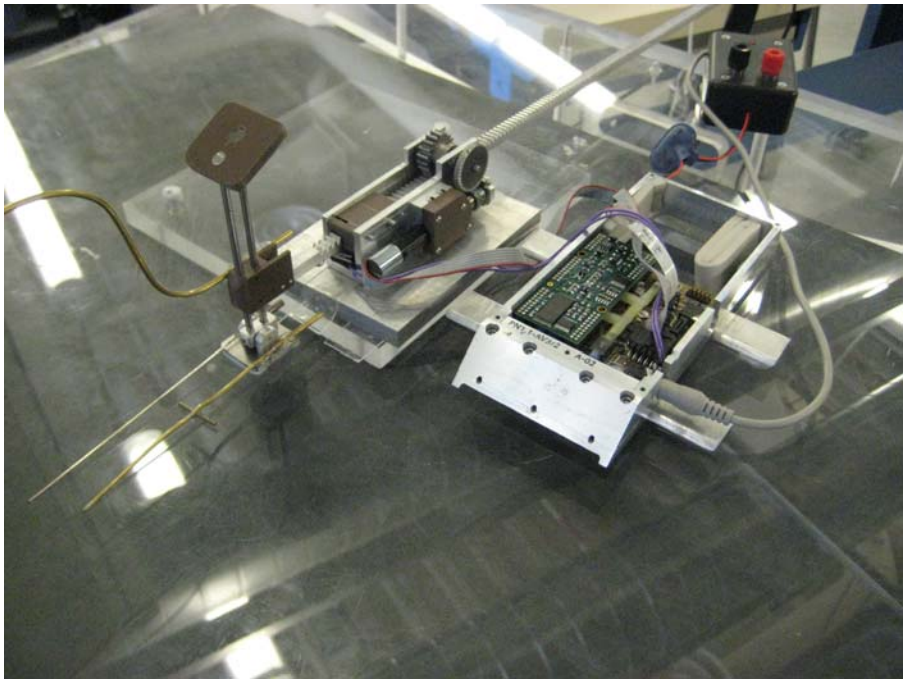

Figure 4.2- Final Assembly next to BLDS

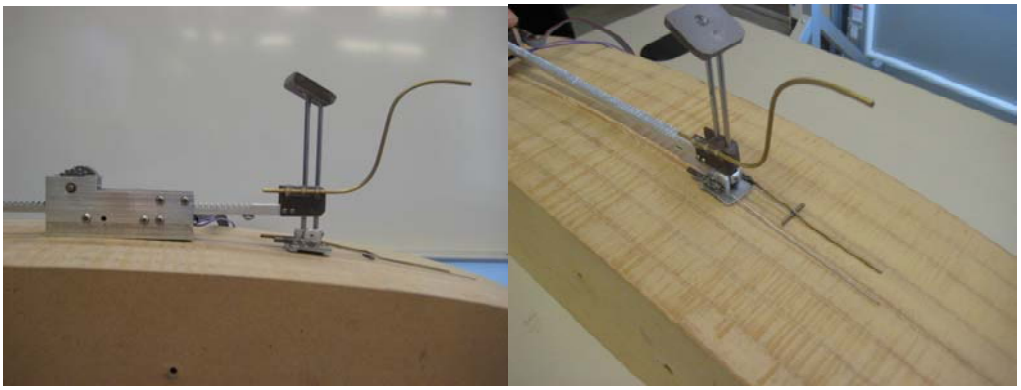

Figure 15 - Final Assembly on Air Foil Model

Design Verification Plan (TESTING)

Stiction Testing

We attached a bucket to the end of the rack and added water until stiction was overcome in order to test what force would cause the rack to begin moving. We found that our system could handle 0.5 ± 0.2 pounds of force. This proves that a braking mechanism will be needed. The current BLDS H-bridge motor control does not provide motor breaking and it is recommended that the BLDS board be redesigned to include breaking or a mechanical breaking system needs to be incorporated to our system.

Table 5.1. Stiction Testing

Iteration II 20/20 Helical Gears					Iteration III -20/40 Helical Gears	
Run	No Grease Forward	Grease Forwards	Grease Backwards		Run	Weight [lbs]
1	430	299	305		1	0.69
2	286	295	238		2	0.39
3	265	321	345		3	0.66
4	332	229	340		4	0.73
5	437	-	-		5	0.69
6	521	-	-		6	0.73
Avg. [grams]	378.5	286	307		Avg. [lbs]	0.648
Avg. [lb]	0.83	0.63	0.68			

Confirmed Final Weight

Our final design weight is within 3.8% of our design requirement. This is within a normal range of the design weight and would require a reasonable amount of tape to hold our entire assembly to the aircraft. By providing enough tape area, a factor of safety will ensure the device will remain attached. See Appendix F for the required tape calculations. The weight meets FAA regulations stating that if the device were to fail and become unattached, an object over 1 pound is a catastrophic failure and is highly dangerous (under 1 pound is considered safe and is common).

Table 4.2 Final Design Weight Table

Predicted Weight	Final Design Weight	Amount of tape required
188.5 Grams 0.41 Pounds	235 Grams 0.52 Pounds	5.0 Inches^2

Bench Testing of Different Foot Iterations

We tested the torsion spring iteration and concluded that there would be too much error introduced to the position calculation. Both spring iterations (extension, torsion) gave undesirable deflection of the rack which caused the system to bind and the motor stalled. The aero fin design proved to be sufficient in the wind tunnel and did not cause the system to bind and fail. The added frontal area was not significant enough to deem the concept unreasonable as the stiction would already be overcome with the previous designs and the amount of extra tape was minimal, about .04 inches squared.

Final Foot Design Results

- Our foot assembly successfully traverses over moderate curvatures and holds the probes against the surface.
- For sections with large curvatures, we found that the orientation of the base drive system is crucial in order to prevent the rack from interfering with the maximum curve peaks for convex curvatures and additional shims will be needed for the extreme curvatures.
- Wind loads at low speeds in the wind tunnel proved to hold the probes against the surface.

Wind Tunnel Observation

On May 28th, we tested our final design in the fluids lab wind tunnel. The purpose of this test was to observe how the assembly would react under high wind speeds. The base was taped in the observation testing area as seen in the figure below and the wind tunnel was run at several different speeds including maximum speed (60 Hz, 110 mph).

Key observations:

- Our device withstood wind tunnel maximum wind speeds (110mph).
- No extreme vibrations at full extension of rack (not deflected or oscillated).
- The rack was not moved back due to wind loads.
- The maximum wind loads seen in the tunnel was only 30 psf, only 1/5th of our design criteria.
- A larger wind tunnel or another method is necessary to test the actual forces our design would see during flight.

Figure 5.1 - Wind Tunnel Test Setup

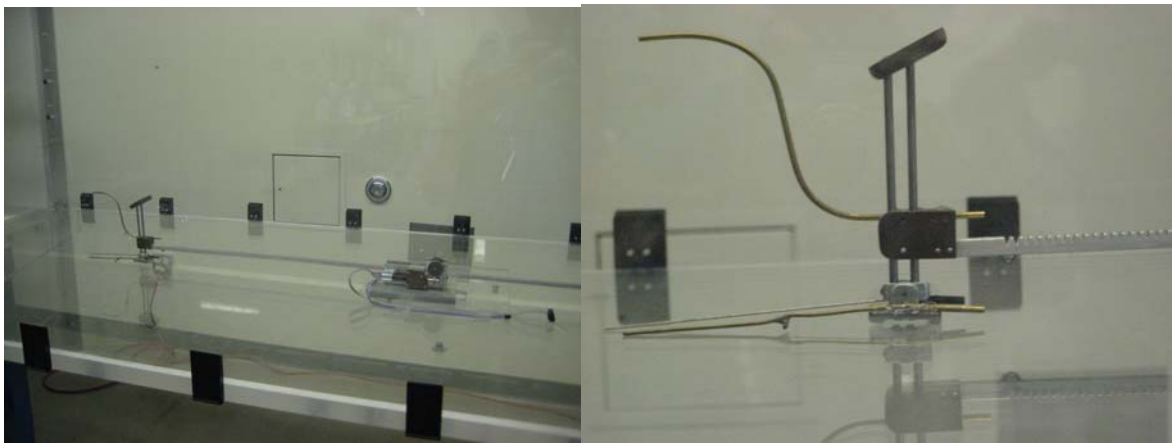

Figure 5.2 - Wind Tunnel Full Flow Testing

Probe Travel Speed/ Accuracy

- The motor, helical gears and rack & pinion components give us an optimal traveling speed for data collection.
- The motor's encoder has 10 counts per revolution and we are able to move between desired data points in a sufficient amount of time. Total length of travel is 33,000 counts and 1 mm is 66 counts.
- Probe traversing speed between 5 and 20 millimeters per second.
- Encoder records position accurate to a millimeter.

Management Plan

Table 6.1 Roles and Responsibilities

Josh Bugni	**Andrew Sofranko**
Overseer of CAD Modeling	Overseer of Components
Machining	Sponsor Liaison
Analysis	Documentation
Records Minutes	Scheduling

Table 6.1 lists the roles and responsibilities assigned to each project partner. The workloads were distributed evenly between the two partners and a lot of the work was done together due to only two members. The individual assignments were in place to ensure smooth working conditions and provided assurance that deliverables for the specific assignments listed above were turned in on time. A full summary of our Gantt chart is provided in the Appendix E. This chart provided us with a schedule and pace to ensure the project finished on time.

Table 6.2 Final Prototype Specification Summary

Weight	**Cost**	**Speed (Max)**	**Traversing Length**	**Tape Required**
.52 Lbs	$493.16	50mm/sec	500 mm	5.0 in^2

Recommendation Summary

Rack Construction

- A 40 degree chamfer tool is a sufficient method for constructing a rack for our purposes.
- The tool path should approach from each side to ensure proper tooth symmetry.
- Aluminum provides a rigid enough structure without too much weight.

Gears

- A pitch of 32 for the rack and pinion gears is a sufficiently small size that has little to no backlash compared to the design accuracy of 1mm.
- Helical gears
    - A pitch of 64 is moderately difficult to align the pitch circles and can cause some issues when they are not within desired location to align pitch circles as such.
        - Further apart then desired causes minimal backlash of approximately half a millimeter of error for the probes but still operates normally.
        - An interference clearance causes binding in the gears that is difficult for the motor to overcome.
- The gear head that came with the motor provided to us works adequately.

Rack Alignment and Positioning

- Rollers are difficult when contacting the tooth side of the rack. They cause too much friction that the motors cannot overcome.
- The sleeve design holds the rack in proper alignment for operation without moving parts and Delrin provides a well lubricated surface with a stiffness that can withstand the wind loads that is transmitted by the rack.

Surface Contact Method

- Springs are unsuitable for providing a force that keeps the foot against the surface because they create an equal and opposite reaction on the rack that adds friction to the system that the motor cannot overcome.
- A torsion spring single joint armature has an error associated with it that is unknown due to the curvature being unknown.

- Angled Aero Fin
    - provides a sufficient force to keep the foot against the surface without adding stiction to the system
    - The added frontal projected area from the fin adds to the force pushing the rack while the probes are in idle position for data acquisition; although, the force without the fin already overcomes the stiction in the system and the added force will not cause the motor to stall.
- The dual linear shaft design provides adequate positioning that is accurate.

Foot assembly

- The pivoted foot assembly provides surface contact at the tip of the probes for moderate curvatures.
- The further back that the probes are mounted relative to the pivot provides a better contact on downward slopped sections.

Design for Minimum Temperature condition

- The moving parts of our system are easily designed with extra clearance, at room temperature, so that the minimum temperatures do not cause the system to bind
- The components required by our design are easy to purchase with temperature ratings within our design range

Future Build Critical Tolerances

- Alignment of helical gears with pillow block and motor mount
- Rack Tip attachment. Use more screws or larger screws.
- Sleeve alignment. We used sand paper attached to a surface to create parallel surfaces between the two sleeves.
- With the dual shafts in the surface contact design, the spacing between the two holes for each part is critical in order to insure smooth motion.
- A sloped surface for the foot assembly to allow probes to angle downward towards surface would be desirable.

Appendix A Total Skin Friction Derivation

The following derivation of the total skin friction equation is shown to mathematically illustrate why a traversing probe is superior to a static probe. The main idea we want to express here is that skin friction will depend on the location along the chord. By knowing the development of the skin friction, it will be easier to understand how the flow is developing and were the transition is occurring. With single data points measured with the static assemblies, it is difficult to understand what the value means between the few data points collected since flow development is not revealed.

Definition of skin friction

$$\frac{\tau_W}{\frac{1}{2}\rho U^2} = \frac{.0594}{(Re_x)^{1/5}} \tag{1}$$

Solving for the shear tress at the wall τ_W

$$\tau_W = \frac{1}{2}\rho U^2 \frac{.0594}{(Re_x)^{1/5}} \tag{2}$$

By integrating the shear stress, total skin friction is found

$$Total\ Skin\ friction = \int_{Leading\ edge}^{trailing\ edge} \tau_W \tag{3}$$

Reynolds number depends on density, free stream speed, position and viscosity

$$Re = \frac{\rho U x}{\mu} \tag{4}$$

Substituting equation (1) and (4) into (3)

$$total\ Skin\ friction = \int_{Leading\ edge}^{trailing\ edge} \frac{2 * .0594 * \rho U^2}{\left(\frac{\rho U x}{\mu}\right)^{1/5}} \tag{5}$$

X is the only variable that depends on position. The rest of the variables can be factored out of the integral.

$$total\ Skin\ friction = .1188\ \frac{\rho U^2}{\left(\frac{\rho U}{\mu}\right)^{1/5}} \int_{Leading\ edge}^{trailing\ edge} \frac{1}{(x)^{1/5}} \tag{6}$$

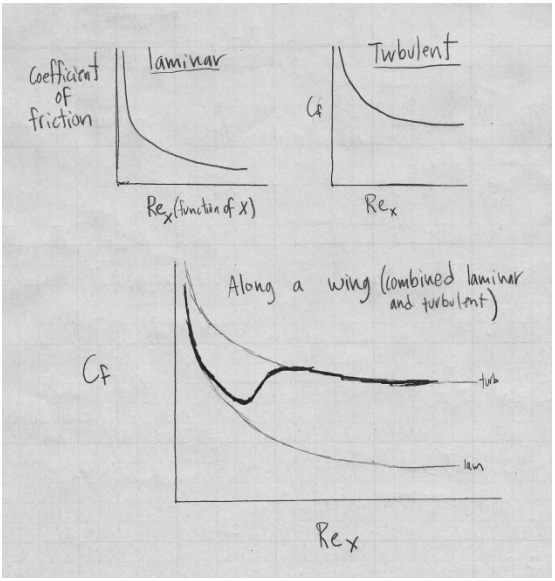

Table A.1 – Skin Friction as a function of Position and Flow Regime

Appendix B Proposed Probe Orientation on Wing Profile

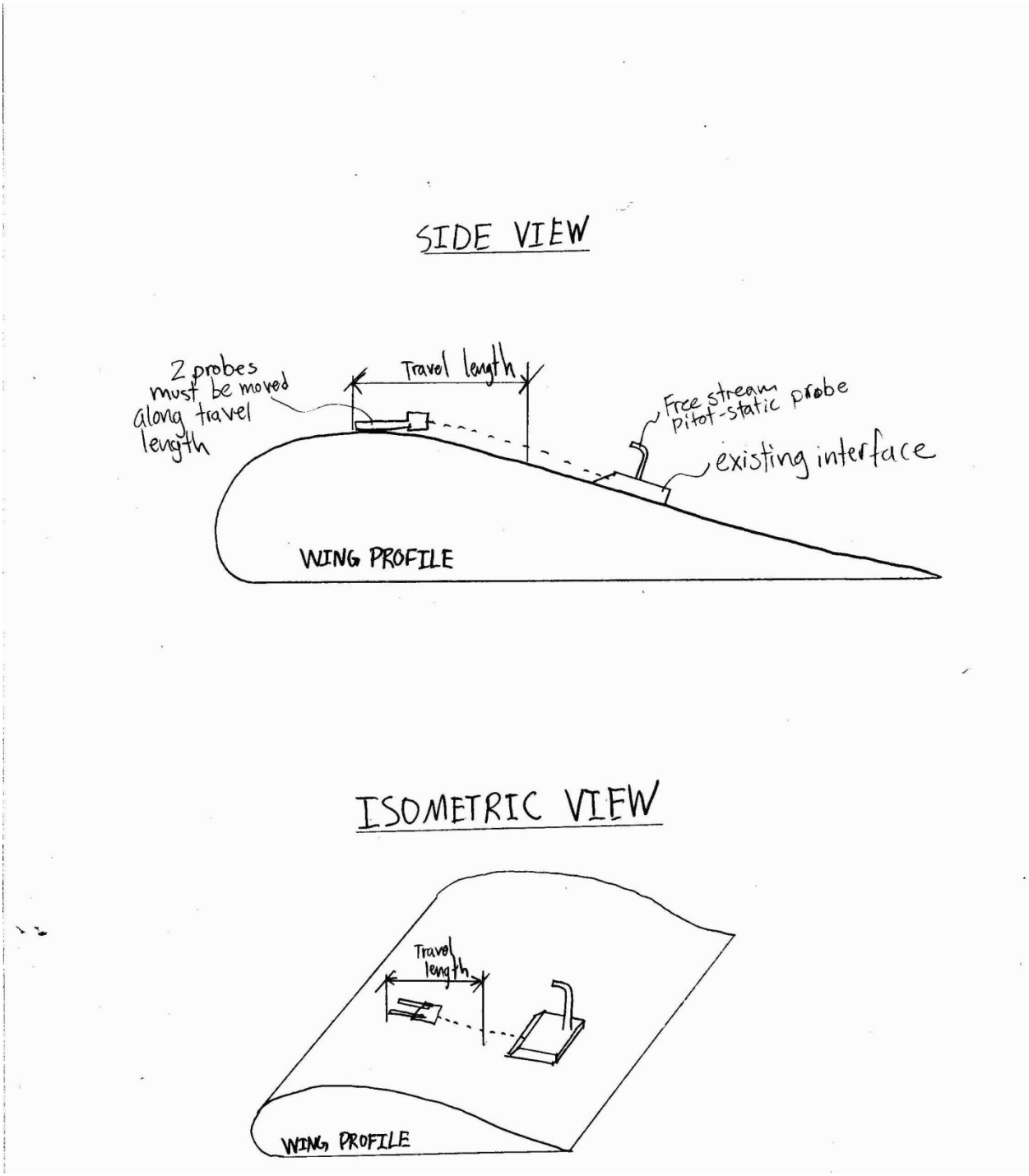

Appendix C Prototype Brain Storming

A model was built out of wood and hardware materials. Our goal was to make a model that would show us how the assembly would sit on the wing and how a rigid arm with a pivot arm and foot would keep the probe on the surface.

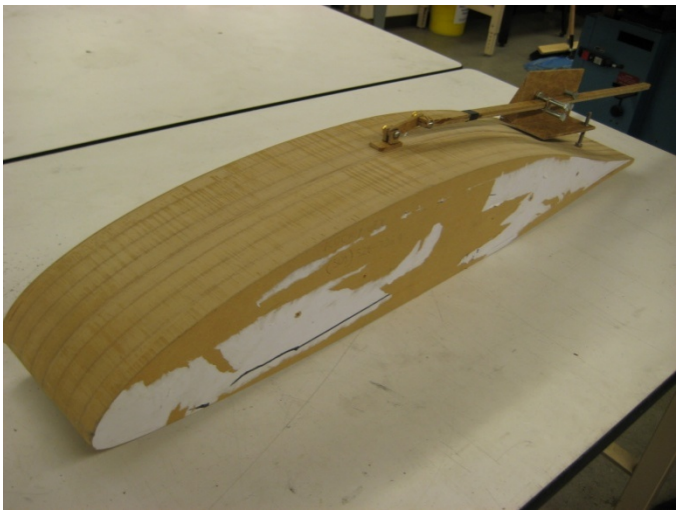

Figure C.1 Model assembly oriented on the back of a model wing.

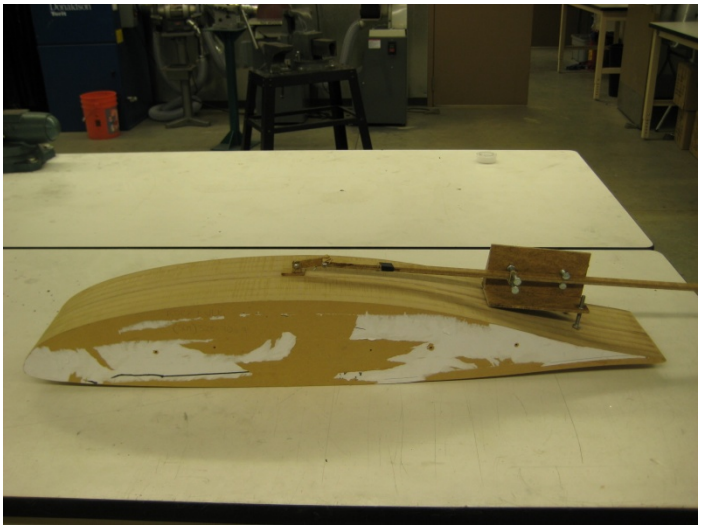

Figure C.2

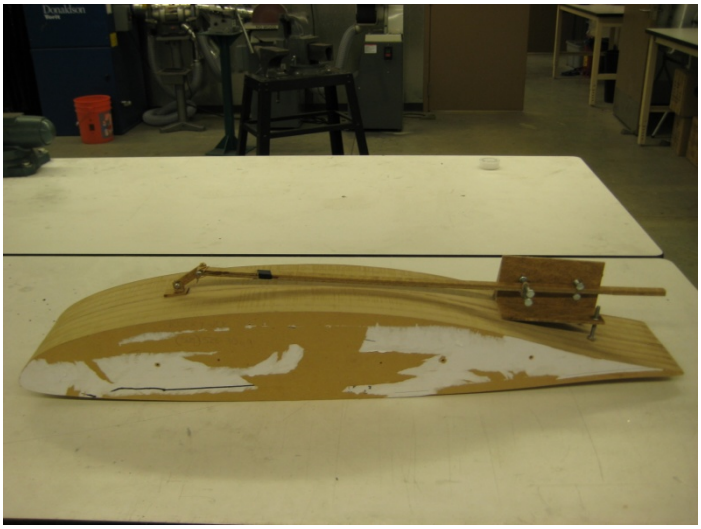

Figure C.3

Figure C.2 and C.3 are side views of the model assembly and wing. This depicts how the pivoting arm keeps the probe foot flush on the surface over the entire surface of the wing.

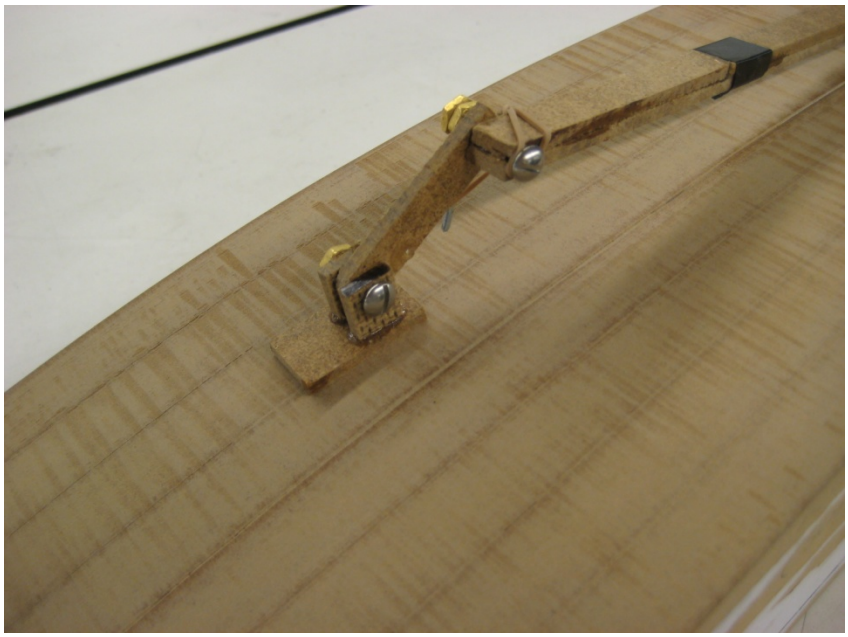

Figure C.4

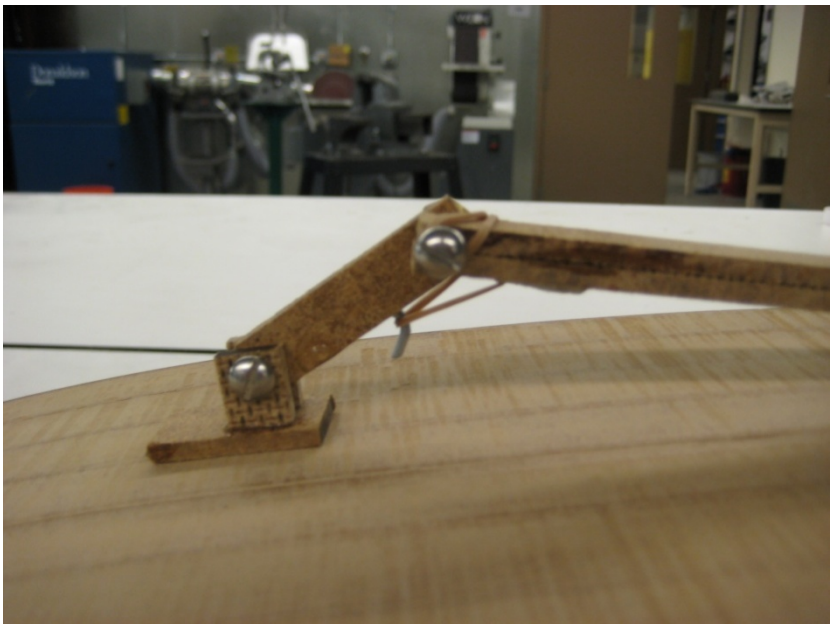

Figure C.5

Figure C.4 and C.5 are close up pictures of the front of the rack arm. A pivot arm attached to the rack will press the foot against the wing with a torsion spring. The foot can also rotate to accommodate all surfaces of the wing. The probes will be mounted on the foot.

Appendix D Rapid Prototype

Shown below is the actual size high density prototype model of our final design for the traversing probe mechanism.

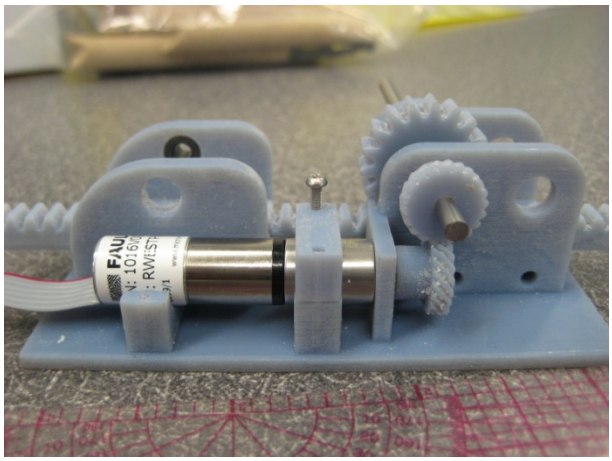

Figure D.1

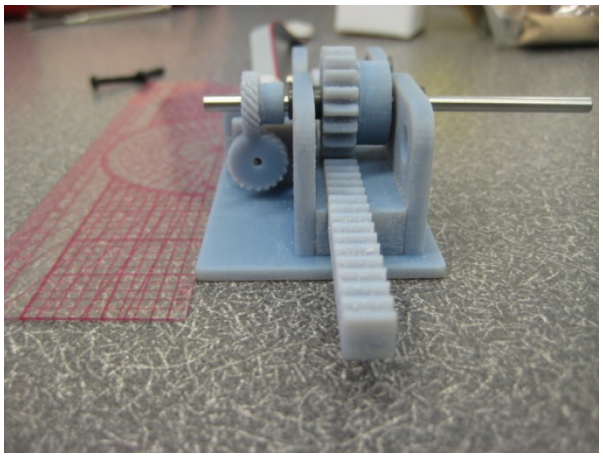

Figure D.2

Figure D.1 and D.2 show the side and front view with the motor attached. An engineering ruler is shown for scale.

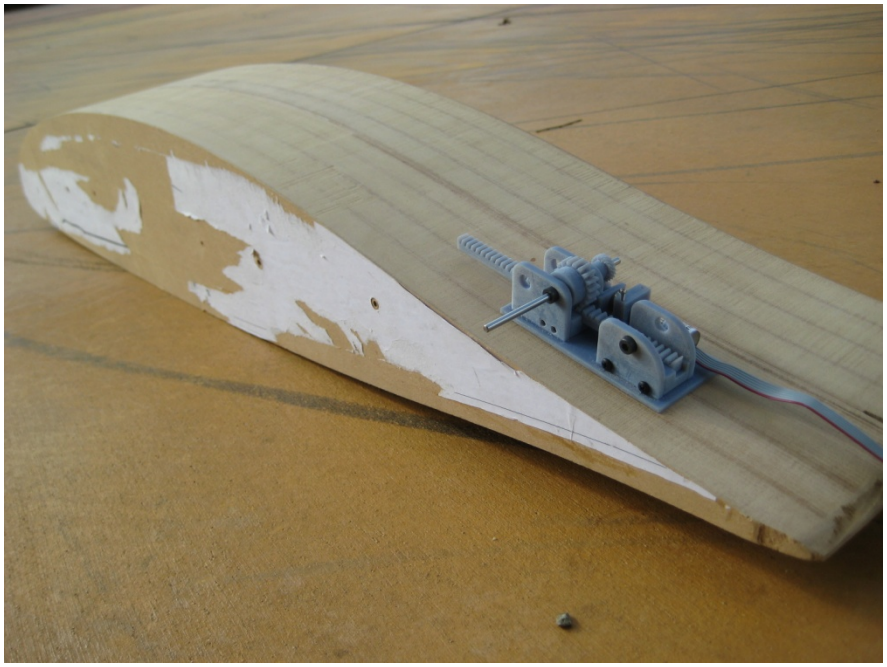

Figure D.3 shows the prototype oriented on the back of the model wing.

Appendix E - Gannt Chart Dates

Meet Group	1 day	Tue 9/29/09	Tue 9/29/09
Meet Sponsor	1 day	Thu 10/1/09	Thu 10/1/09
Objective Brainstorm	1 day	Thu 10/8/09	Thu 10/8/09
Meeting With Sponsor	1 day	Thu 10/8/09	Thu 10/8/09
Project Report	150 days	Fri 11/6/09	Mon 5/31/10
Yellow/Red Tag Certification	1 day	Sat 10/10/09	Sat 10/10/09
Project Proposal / Requirements Document	8 days	Wed 10/7/09	Thu 10/15/09
Detailed Schedule	8 days	Tue 10/13/09	Thu 10/22/09
Concept Design	11 days	Thu 10/15/09	Thu 10/29/09
Decision Matrix	1 day	Tue 10/27/09	Tue 10/27/09
Design Selection	6 days	Tue 10/27/09	Tue 11/3/09
Concept Design review	1 day	Tue 11/3/09	Tue 11/3/09
Detailed Design	23 days	Fri 10/30/09	Tue 12/1/09
Drive Box Design	23 days	Fri 10/30/09	Tue 12/1/09
Arm Design	23 days	Fri 10/30/09	Tue 12/1/09
Wing Contact Design	23 days	Fri 10/30/09	Tue 12/1/09
Concept Design Report	13 days	Tue 10/20/09	Thu 11/5/09
Prototype Concepts	7 days	Thu 11/5/09	Fri 11/13/09
In Class Design Review	1 day	Tue 11/17/09	Tue 11/17/09
428 Design Report	1 day	Tue 12/1/09	Tue 12/1/09
Meet with Sponsor	1 day	Thu 12/3/09	Thu 12/3/09
Finalize Design	5 days	Mon 1/4/10	Fri 1/8/10
Order final parts	1 day	Fri 1/8/10	Fri 1/8/10
Build	93 days	Wed 1/20/10	Wed 5/26/10
Build Iteration I	34 days	Wed 1/20/10	Sun 3/7/10
Machine Aluminum Rack	2 days	Fri 1/22/10	Mon 1/25/10
Build Iteration II	8 days	Fri 5/7/10	Mon 5/17/10
Build Iteration III	8 days	Mon 5/17/10	Wed 5/26/10
Test	14 days	Sun 5/9/10	Wed 5/26/10
Stiction Testing	1 day	Sun 5/9/10	Sun 5/9/10
Bench Model Test	4 days	Fri 5/21/10	Wed 5/26/10
Wind Tunnel Test	1 day	Wed 5/26/10	Wed 5/26/10
Expo	1 day	Thu 5/27/10	Thu 5/27/10
Final Report & Hardware Turned In	1 day	Fri 6/3/10	Fri 6/3/10

Appendix F

Analysis

Drag Force on Rack
Before build estimate

Drag Force

$F_d = \frac{1}{2} C \rho U^2 A$ assume $C = 1$

$F_d = \frac{1}{2}(1)\rho\left(400\frac{ft}{s}\right)^2 A$

ρ_{air} @ 30,000 ft $= .000889 \frac{lb}{ft^3}$ ρ_{air} @ 10,000 ft $= .001755 \frac{lb}{ft^3}$

$F_d = \frac{1}{2}(1)\left(.000889\frac{lb}{ft^3}\right)\left(400\frac{ft}{s}\right)^2 A$ $F_d = \frac{1}{2}(1)(.001755)(400)^2 A$

30K Altitude: $F_d = 71.1\ psf \cdot A$

10K altitude: $F_d = 140.4\ psf \cdot A$

Conservative: $F_d = 200\ psf \cdot A$

A:

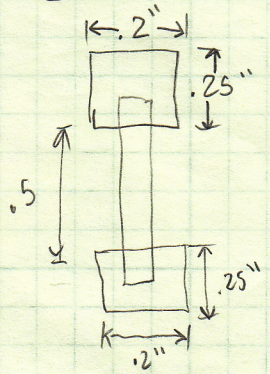

$A = .1\ in^2$

$F_d = 200psf\,(.1\ in^2)\frac{1\ ft^2}{144\ in^2}$

$F_d = .139\ lb$

$T_{pinion} = F \cdot R$

$T_p = (.1391b)(.375\ in)$

$T_p = .0521\ in\ lb$

$T_p = 5.88\ mNm$

used for Gear stress analysis

$HP = \frac{T[ft\cdot lb]\,2\pi\,w(rpm)}{33000}$

$T_p = .0521\ in\ lb = .00434\ ft\cdot lb$

$HP = (.00434)\,2\pi\,(1436)/33000$

$HP = 1.18\times10^{-5}$

Torque seen by motor: $T_{motor} = T_p N$

$T_m = 5.88 mNm\left(\frac{1}{1024}\right)$

$T_m = .0057\ mNm$

Motor Stall torque $T_{stall} = 2.89 mNm$

Max torque input to gearhead $T_{Gmax} = 300 mNm$

$T_m \ll T_{stall}$

$.0057 mNm \ll 2.89 mNm$

$T_p \ll T_{Gmax}$

$5.88 \ll 300 mNm$

Frontal Projecte Area of Rack

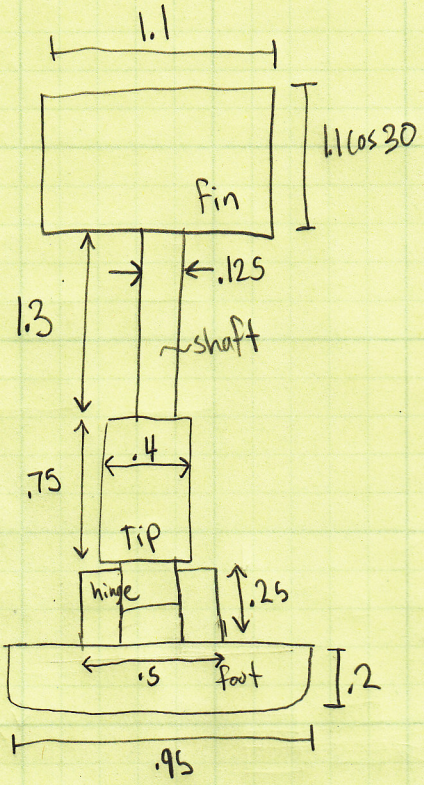

$$Area = (1.1 \times 1.1\cos 30) + (.125)(1.3) + (.4)(.75) + (.25)(.5) + (.2)(.95)$$

$$Area = 1.825\ in^2$$

Conservative

$$F_{drag} = 200\ psf\ (1.825\ in^2)\ \frac{1\ ft^2}{144\ in^2}$$

$$F_{drag} = 2.5\ lbf$$

$$T_{pinion} = (2.5\ lb)(.375\ in)$$

$$T_p = .9375\ in{\cdot}lb$$

$$T_p = 0.1059\ Nm$$

$$T_{motor} = T_p N$$

$$T_m = 0.1059\ Nm\ \left(\frac{1}{64}\ \frac{1}{2}\right)$$

$$T_m = .83\ mNm$$

Torque seen by motor at max speed - Conservative value

Operating

$$F_{drag} = 150\ (1.825\ in^2)\ \frac{1\ ft^2}{144\ in^2}$$

$$F_{drag} = 1.9\ lbf$$

$$T_{pinion} = (1.9\ lb)(.375\ in)$$

$$T_p = .7125\ in{\cdot}lb$$

$$T_p = .0805\ Nm$$

$$T_m = 0.0805\ Nm\ \left(\frac{1}{64}\ \frac{1}{2}\right)$$

$$T_m = .63\ mNm$$

Stall torque of motor $T_{stall} = 2.89\ mNm$

Torque seen by motor is 3.5 times smaller then the torque caused by maximum wind loads.

Forces on Angled Fin

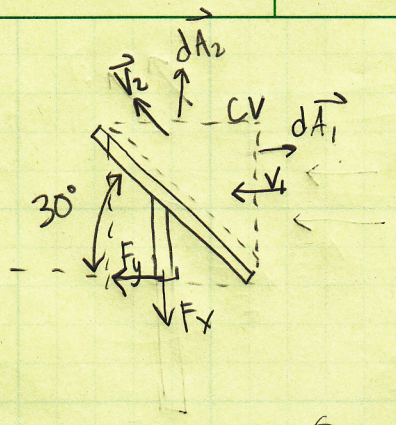

$\rho \approx .00234 \frac{lbf\ s^2}{ft^4}$ standard sea level

$dA_2 = 1'' \times 1 \cos 30'' = \frac{\sqrt{3}}{2} in = \frac{\sqrt{3}}{24} ft$

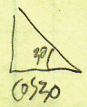

$$\sum F = \frac{\partial}{\partial t}\int_{cv} \vec{V}\rho\, dV + \int_{cs1} \vec{V}_1 \rho \vec{V}_1 \cdot d\vec{A}_1 + \int_{cs2} \vec{V}_2 \rho \vec{V}_2 \cdot d\vec{A}_2$$

(+) (−)

from momentum flux

$F_y = \sin(30)\, V^2 \rho A$

$F_y = \sin(30) .00234 \frac{lbf\ s^2}{ft^4} \frac{\sqrt{3}}{24} ft^2 \left(V \frac{ft}{s}\right)^2$

$F_y = 8.44 \times 10^{-5}\ V^2\ lbf$

Assume $C = 1.6$ (triangle → equalateral) (conservative)

$F_x = F_{drag} = \frac{1}{2} \rho V^2 C A$

$F_x = \frac{1}{2}\left(.00234 \frac{lbf\ s^2}{ft^4}\right)(1.6)\left(V \frac{ft}{s}\right)^2$

$F_x = .001872\ V^2 A\ [lbf]$

F_y = Pressure × Area (cos(30)) F_x = Pressure $\frac{lb}{ft^2}$ × Area in^2 $\frac{1\ ft^2}{144\ in^2}$

Pressure = 30 psf (wind tunnel max) ?! 150 psf (design condition max)

from momentum flux

$F_{y\ wind\ tunnel} = .013\ lbf$

$F_{y\ design\ max} = .07\ lbf$

from drag force w/ $C = 1.6$

$F_{x\ wind\ tunnel} = .025\ lbf$

$F_{x\ design\ max} = .12\ lbf$

} force added due to fin

Probe Speed for Motor Selection

DESIRED PROBE (RACK) SPEED

$> 2 \frac{mm}{sec}$ Shoot for $10 \frac{mm}{sec}$

$V_{rack} = 10 \frac{mm}{sec} = 23.6 \frac{in}{min}$

$R = \frac{.75}{2} = .375$

$V = \omega R$

$\omega = V/R$

$\omega = \frac{23.6 \frac{in}{min}}{.375 \text{ in}}$

$\omega = 63 \frac{rad}{min} \frac{1 \text{ rev}}{2\pi \text{ rad}}$

$\omega_{pinion} = 10 \text{ rpm}$ desired

ACTUAL PROBE SPEED

$N_{desired} = \frac{\omega_{motor}}{\omega_{pinion}} = \frac{14\,700 \text{ rpm}}{10 \text{ rpm}} = 1470$

Select Gear head with gear down 1024:1

Micromo 1024 -012 S

$\omega_{pinion} = N_{Gearhead} \cdot \omega_{motor}$

$\omega_{pinion} = \frac{1}{1024} \cdot (14700 \text{ rpm})$

$\omega_{pinion} = 14.36 \text{ rpm}$

$\frac{1}{64}(14700)$

$\omega_p = 230 \text{ rpm}$

$\omega = 1150$

$V_{rack/probe} = R\omega$

$V_r = (.375 \text{ in})(14.36 \frac{rev}{min} \frac{2\pi \text{ rad}}{1 \text{ rev}})$

$V_r = 33.8 \frac{in}{min}$

$V_r = 14.3 \frac{mm}{s}$

30 sec -

15-sec - 32084 tics 10/rev

$\frac{70}{30} \frac{rev}{sec} = 2.3 \frac{rev}{sec}$

60 sec

10-sec - 21134

10- - 22345

Actual Speed

motor run @ 10V

.2 amps

$V = r\Omega$

$K = 2231 \frac{rpm}{V} \times 5v = 11155\ rpm$

$\Omega_{motor} = 11155\ rpm$

$V_{mass} = \frac{1}{64}\frac{1}{2}(.75\ in)11155\ \frac{rev}{min}$

$V_{mass} = 65 \left[\frac{in}{min}\right]\frac{1m}{60s}\cdot\frac{25.4\ mm}{1\ in}$

$V = 27.7\ \frac{mm}{sec}$

Position

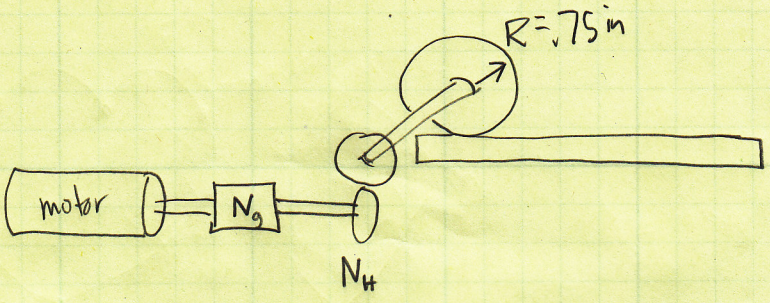

$V = r\Omega$

$X = r\theta$

$$\theta_m = N_g N_H \frac{X}{r}$$

$$\theta_m[\text{rev}]\left[\frac{10 \text{ encoder ticks}}{1 \text{ rev}}\right] = \frac{1}{64}\frac{1}{2}\frac{X \text{ in}}{.75 \text{ in}}$$

$$X = \frac{1}{64}\frac{1}{2}\frac{1}{10 \text{ encoder ticks}}.75 \text{ in} = 5.859\times10^{-4}\frac{\text{in}}{1 \text{ encoder tick}}$$

$$X = 5.86\times10^{-4}\frac{\text{in}}{\text{ET}}\cdot\frac{1 \text{ ft}}{12 \text{ in}}\frac{.3048 \text{ m}}{1 \text{ ft}}\frac{1000 \text{ mm}}{1 \text{ m}} = .015 \frac{\text{mm}}{\text{encoder tick}}$$

$$\frac{1 \text{ mm}}{.015 \text{ mm}} = \frac{\text{encoder ticks}}{\text{mm}}$$

$$66\tfrac{2}{3} = \frac{\text{encoder ticks}}{\text{mm}}$$

$$l = 500\text{mm} \times 66\tfrac{2}{3}\frac{\text{ticks}}{\text{mm}}$$

$$l = 33{,}333 \text{ ticks}$$

deflection

$(21.3 \times .15) + .5(21.3 \times .1) = 4.26\ in^2$

$(21.3 \times .25) = 5.325\ in^2$

$F_{side} = 79\ psf \cdot A$ @ 300 ft/s @ 10,000 ft

$F_{side} = .0\ psf\ (5.325\ in^2)$

$F_{side} = 1065\ lbf$

$F(4.26) = 336\ lbf$

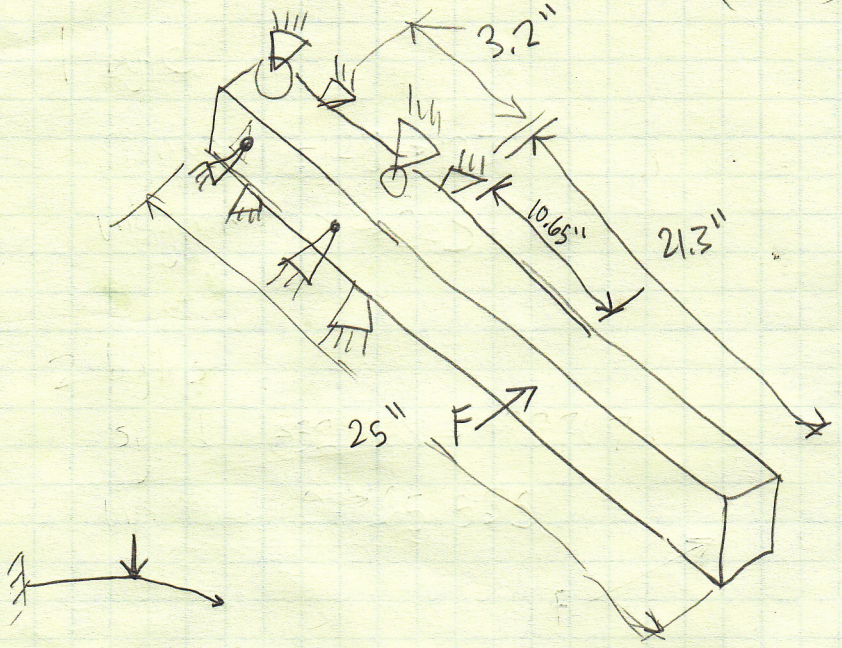

$$\delta_{end} = \frac{5PL^3}{48EI}$$

λ = mode

$$w_n = \sqrt{\frac{EI(L\lambda)^4}{mL}}; \quad \lambda = \frac{\pi}{L}$$

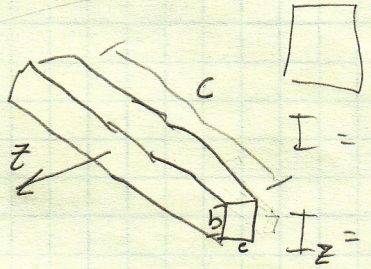

$$I = \frac{h^4}{12}$$

$$I_z = \frac{m}{12}(b^2 + c^2)$$

$$m = \frac{abce}{g}$$

$$m = \frac{(21.3)(25)(.15)(.100\ lb/in^3)\left(\frac{12^3\ in^3}{1\ ft^3}\right)}{32.2\ \frac{ft}{s^2}} = .00248\ slugs$$

$$I_z = \frac{.00248\ slugs}{12}\left(\left(\frac{.15}{12}\right)^2 + \left(\frac{.25}{12}\right)^2\right)$$

$$I_z = 1.22 \times 10^{-7}\ ft^4$$

$$\delta_{max\ yaw\ @300\ ft/s} = \frac{5(336\ lbf)\left(21.3\ \frac{1}{12}\ ft\right)^3}{48(1.526 \times 10^{12}\ psf)(1.22 \times 10^{-7}\ ft^4)} = .00105\ ft$$

$\delta_{max} = .012\ in$

$$E = 10.6 \times 10^9\ \frac{lb}{in^2}\left(\frac{12\ in}{1\ ft}\right)^2 = 1.526 \times 10^{12}\ psf$$

$$w_n = \sqrt{\frac{(1.526 \times 10^{12}\ \frac{lbs}{ft^2})(1.22 \times 10^{-7}\ ft^4)\left(\frac{21.3}{12}\ ft \cdot 1\right)^4}{(.00248\ \frac{lbs\ s^2}{ft})\left(\frac{21.3}{12}\ ft\right)}} = 20490\ \frac{1}{s}$$

High natural frequency good, will most likely not resonate

Design for min Temperature

T_2 = Temperature - -60°C or -76°F

T_1 = 70°F

Sleeve Geometry

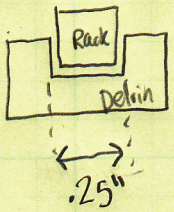

.005in of clearance needed for room temperature operation (friction)

Coefficients of expansion

$\alpha_{delrin} = 4.5\times10^{-5}\ \frac{in}{in\,°F}$

$\alpha_{aluminum} = 12.3\times10^{-7}\ \frac{in}{in\,°F}$

$\alpha_{steel} = 7.3\times10^{-6}\ \frac{in}{in\,°F}$

$\alpha_{Brass} = 10.3\times10^{-6}\ \frac{in}{in\,°F}$

$\Delta l = \alpha\, l_i\, \Delta T$

$\Delta l_{al} = 12.3\times10^{-7}\left(\frac{in}{in\,°F}\right)(.25in)(70--76°F)$

$\Delta l_{al} = .0000449\ in$

$\Delta l_{delrin} = 4.5\times10^{-5}\left(\frac{in}{in\,°F}\right)(.25in)(70--76°F)$

$\Delta l_{delrin} = .00168\ in$

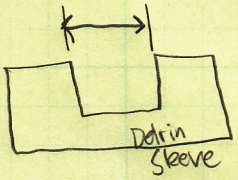

linear shaft

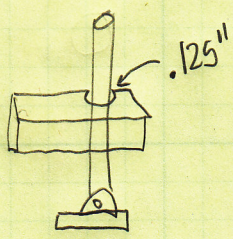

$\Delta l_{steel\ shaft} = 7.3\times10^{-6}\frac{in}{in\,°F}(.125\ in)(146°F)$

$\Delta l_{steel} = .000133\ in$

$\Delta l_{delrin\ hole} = 4.5\times10^{-5}\frac{in}{in\,°F}(.125in)(146°F) = .00082\ in$

hole = .126 in shaft = .125 in

Shaft to bearings

$\Delta l_{steel} = .000133\ in$

$\Delta l_{Brass} = 10.3\times10^{-6}\frac{in}{in\,°F}(.125in)(146°F)$

$\Delta l_{Brass} = .000188\ in$

Brass and Steele will shrink at similar rates

Change stage menu-

```
Stage option 4: //move rack between limits continuously
while (movement$ <> "e" & movement$ <> "E")
    while (Pin(7) <> 0)
        pclr 4   //set direction of rack ____
        pset 2   // turn on motor
    wend
        pclr 2   // stop motor immediately for safety
    while (Pin(6) <> 0)
        pset 4   // set direction of rack ____
        pset 2   // turn on motor
    wend
wend
pclr 2
```

```
Stageoption5: //move rack between limits & pause at a few locations
  increment = ___ //          also pauselength = ____
  while (movement$ <> "e")
      Pset 21
      backcount = 0
      count backcount
      while (Pin(7) <> 0)
          pclr 4   //set dir of rack ____
          Pset 2   //turn on motor
          if (backcount => movement)
          pause
```

```
        :
        if (backcount > increment)
            Pclr 2
            pause = 0
            while (Pause < Pause_length)
                count Pause
            wend
        endif
wend

while (Pin(6) <> 0)
    Pset 4  // set dir of rack ——————
    Pset 2
    if (backcount > increment)
        pclr 2
        pause=0
        while (Pause < pause_length)
            count Pause
        wend
    end if
wend
```

Tape Required Calculations

Here is the reduced required tape calculations completed in Excel. This was a sanity check to confirm that we would have enough area on our assembly to attach it with structural adhesive tape.

Table D1.

Assumptions:
10 degree yaw angle for side drag
Cp = 1
Drag Equation: Fd=.5*C*p*v^2*A
We used: Pressure*A (front area)
(side area)Pressure *sin^2(10)*A
Pressure = 200 or 150 lbf/ft^2
Yaw Factor = 0.03

Weight	0.52
3G	1.56
tape	2.34 in^2 Tape

		Dimensions (in)			in^2	in^2	in^2	200 psf		Tape Required in^2			
	Model #	Height	Length	Width	Area of Rack	Front Area	Side Area	Front Drag	Side Drag	RSS Forces	Drag	Total Tape	
Design I	1	1.225	5.5	1.5	5	1.84	6.74	2.55	0.49	2.60	3.90	6.24	in^2
Design II	2	1.225	3.5	1.5	5	1.84	4.29	2.55	0.39	2.58	3.87	6.21	in^2
Design III	3	1	3.5	1.5	5	1.50	3.50	2.08	0.35	2.11	3.17	5.51	in^2
Interation I. 20 -Jan	4	1.25	3.5	1.65	5	2.06	4.38	2.86	0.39	2.89	4.34	6.68	in^2
Interation II. 7-May	Iteration 2				5	1.044	3.84	1.45	0.37	1.50	2.24	4.58	in^2
Interation III. 17 -May	Final Design				5	1.247169	4.32	1.73	0.39	1.78	2.66	5.00	in^2

Appendix G

Balloon View

Exploded View

Engineering Drawings

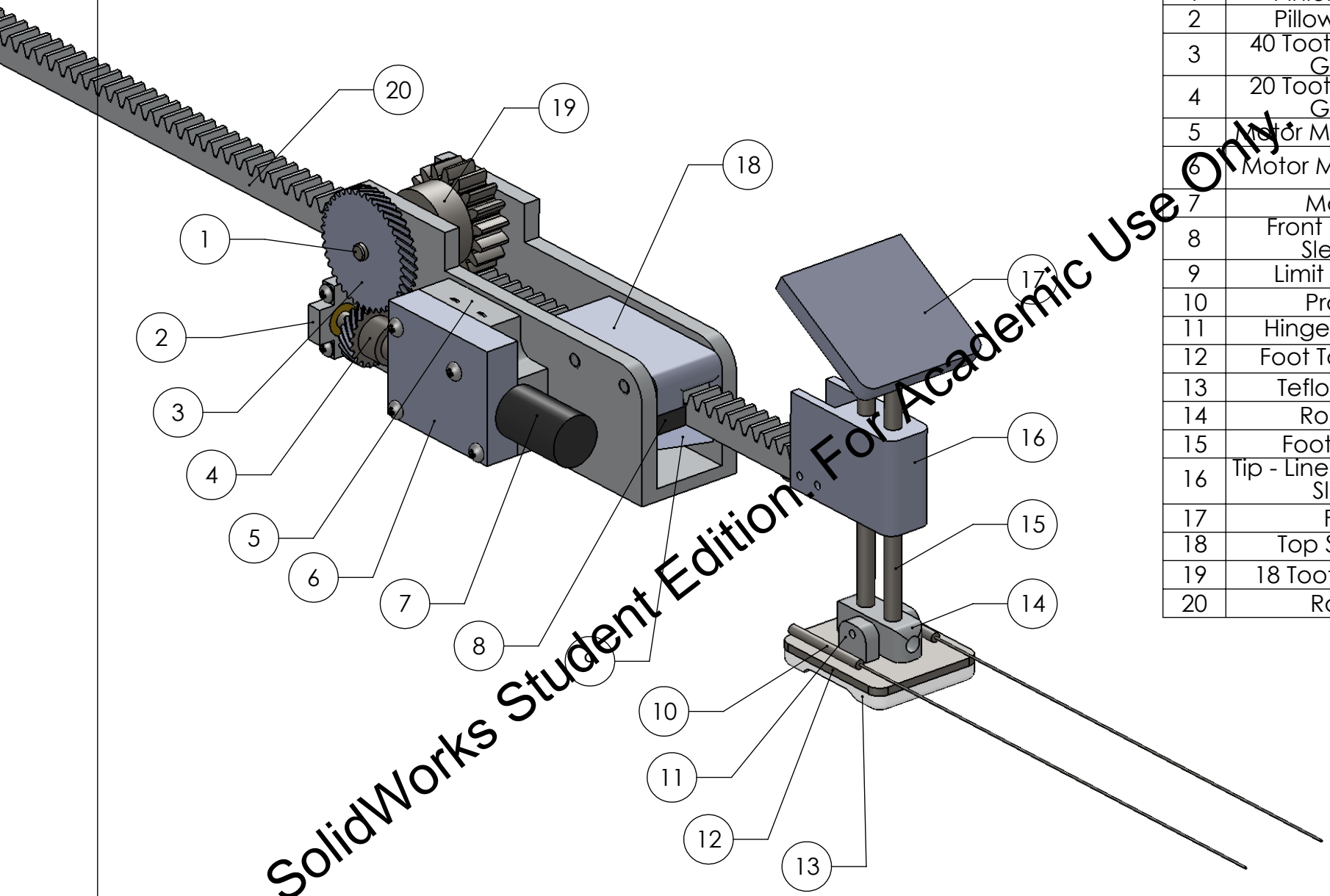

#	Description
1	Pinion Shaft
2	Pillow Block
3	40 Tooth Helical Gear
4	20 Tooth Helical Gear
5	Motor Mount Base
6	Motor Mount Top
7	Motor
8	Front Bottom Sleeve
9	Limit Switch
10	Probe
11	Hinge @ Foot
12	Foot Top Base
13	Teflon Foot
14	Rocker
15	Foot Shaft
16	Tip - Linear Bearing Slide
17	Fin
18	Top Sleeve
19	18 Tooth Pinion
20	Rack

Mechanical Engineering CAL POLY

ME430 Winter 2009	SCALE: 1:1	TITLE: Balloon Assembly
NEXT ASSY:	DATE: 6-3-2010	NAME: Josh Bugni & Andy Sofranko

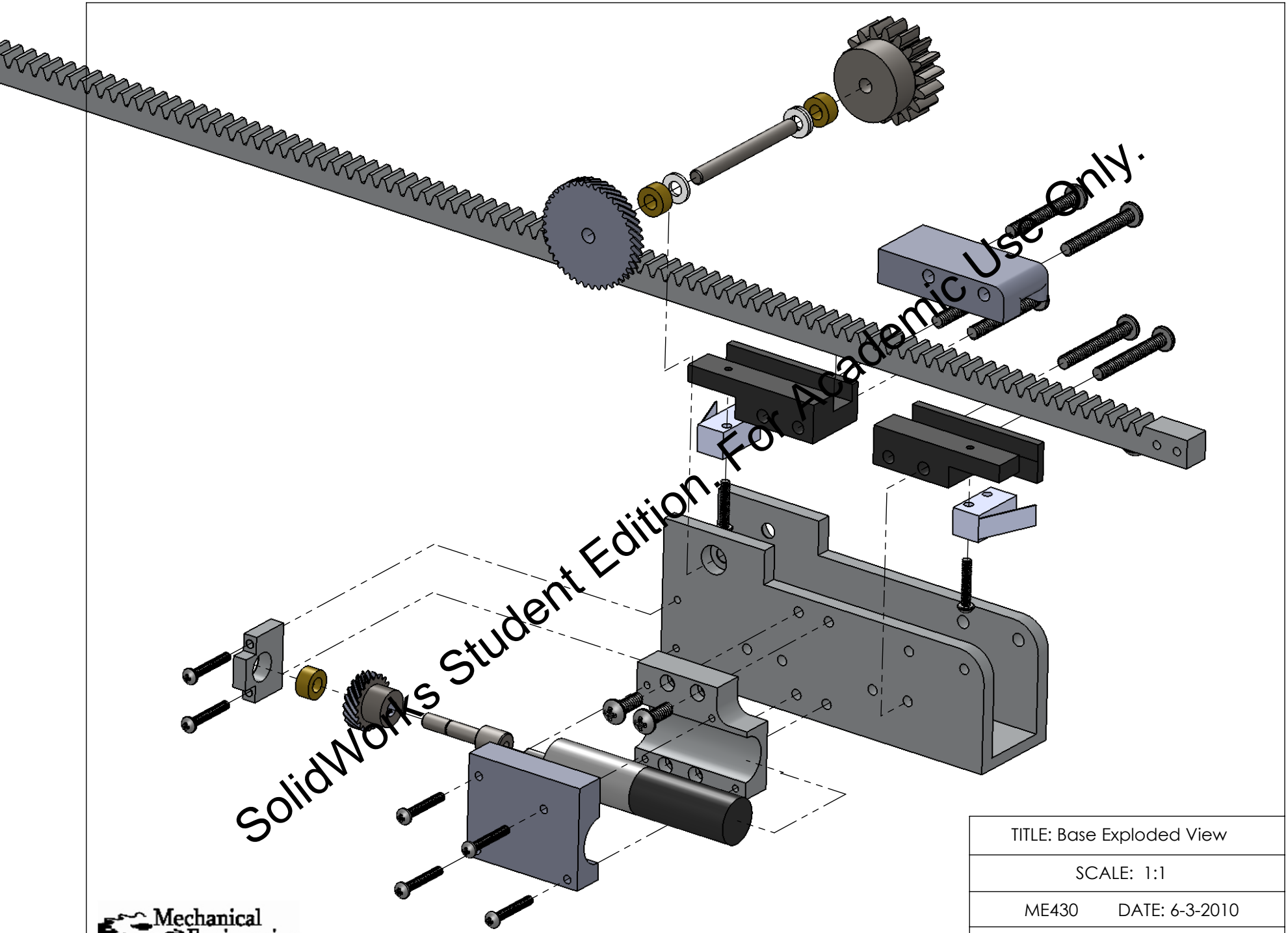

Mechanical Engineering CAL POLY

TITLE: Base Exploded View
SCALE: 1:1
ME430 DATE: 6-3-2010
NAME: Josh Bugni & Andy Sofranko

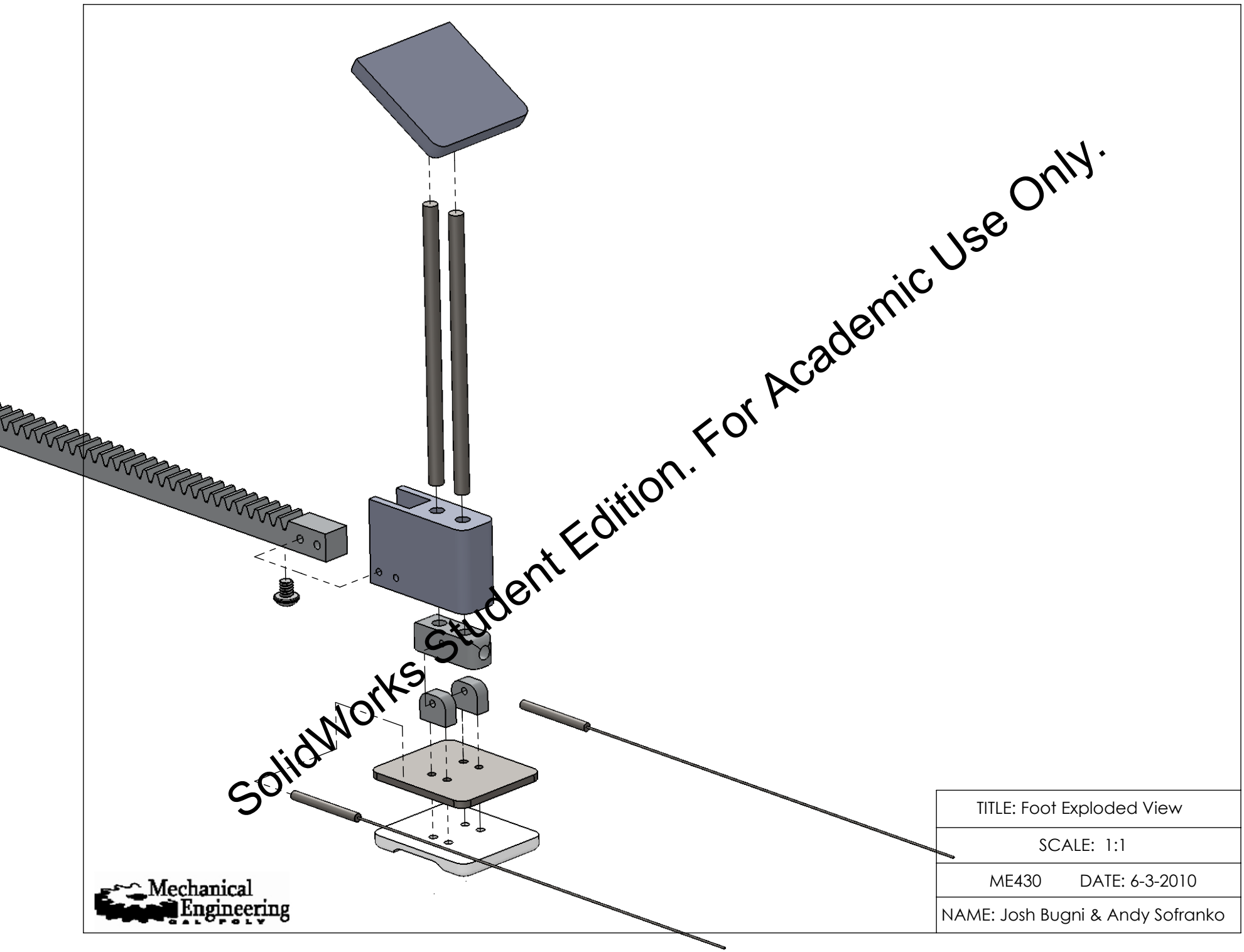

Mechanical Engineering CAL POLY

TITLE: Foot Exploded View
SCALE: 1:1
ME430 DATE: 6-3-2010
NAME: Josh Bugni & Andy Sofranko

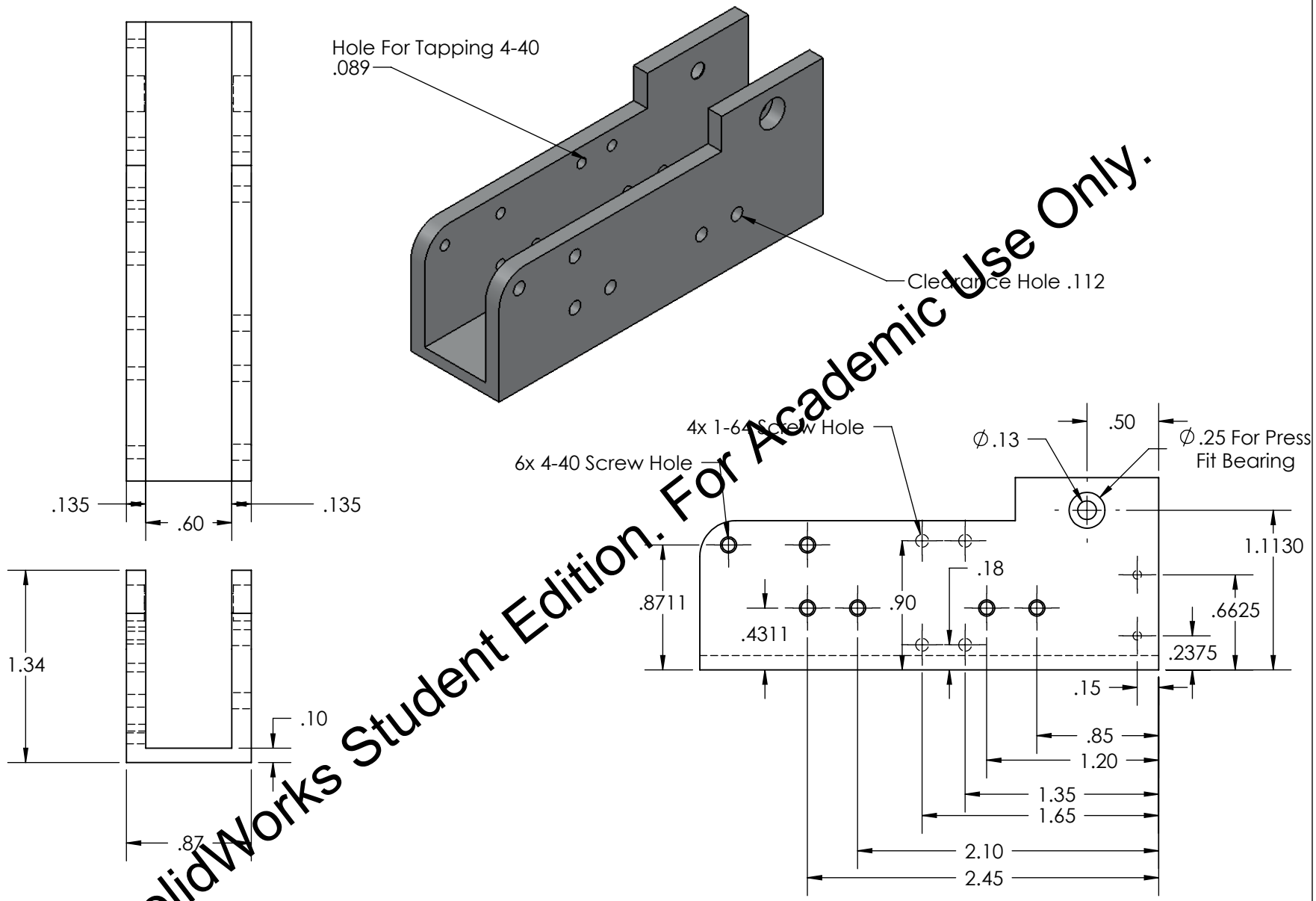

ME429 Winter 2009	TOLERANCE: ±.01	MATERIAL: Alluminum
	SCALE: 1:1	DRAWING #: 004
	UNITS: Inches	TITLE: Base
NEXT ASSY: 005	DATE: 6-4-2010	NAME: Josh Bugni & Andy Sofranko

Mechanical Engineering
CAL POLY

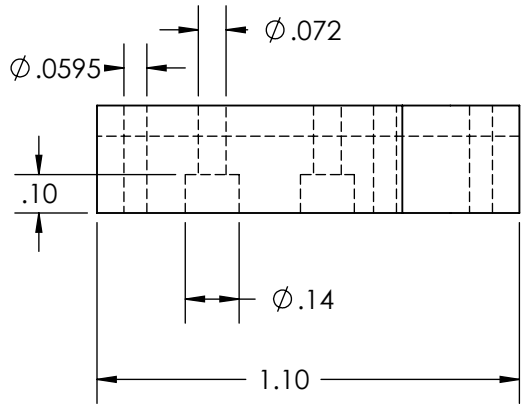

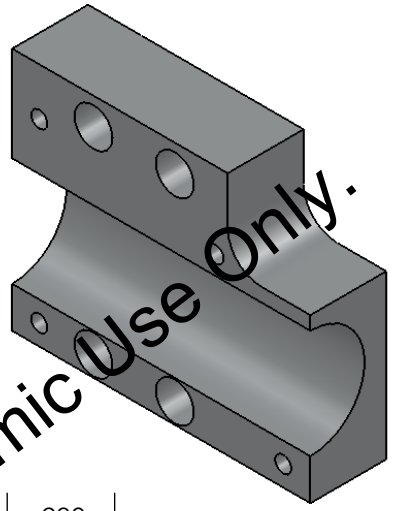

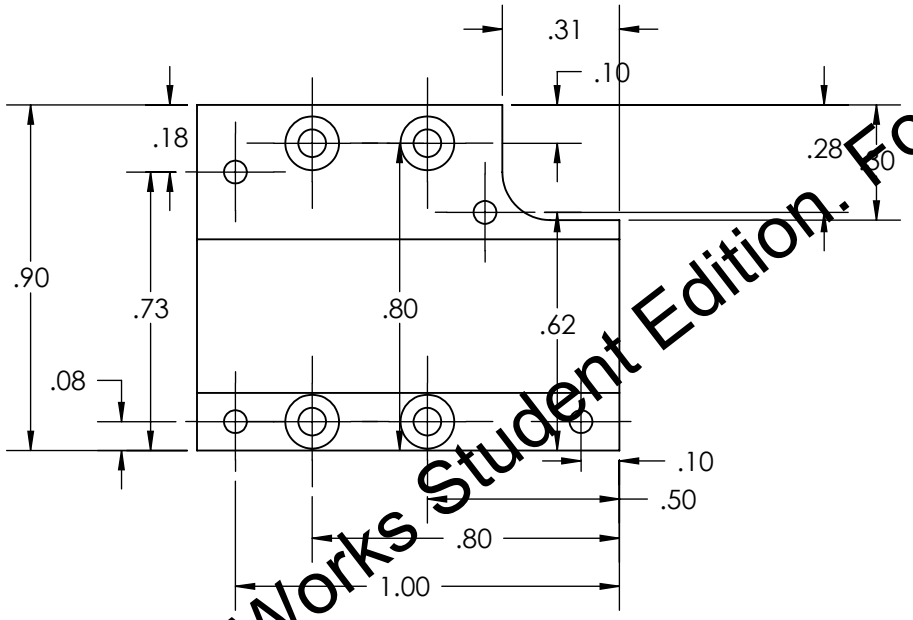

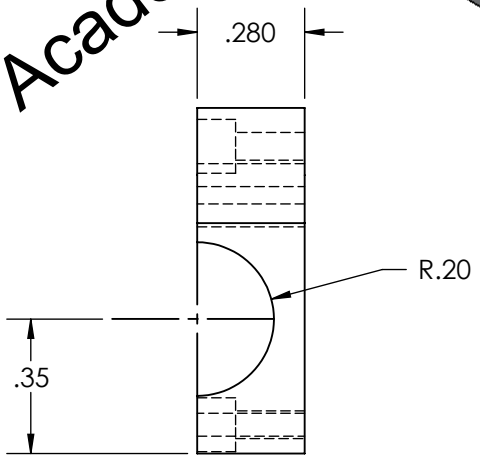

ME430 Winter 2009	TOLERANCE: ±.01	MATERIAL: Alluminum (6061 Alloy)
	SCALE: 2:1	DRAWING #: 005
	UNITS: Inches	TITLE: Motor Mount Base
NEXT ASSY: 006	DATE: 6-4-2010	NAME: Josh Bugni & Andy Sofranko

Mechanical Engineering
CAL POLY

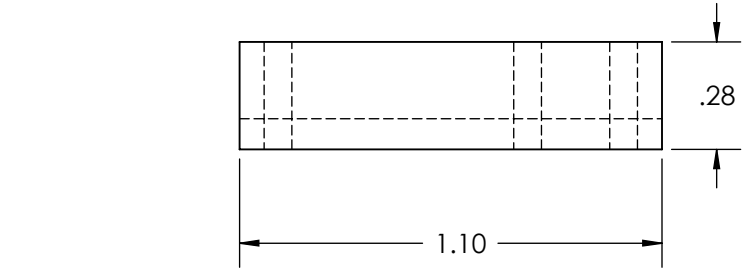

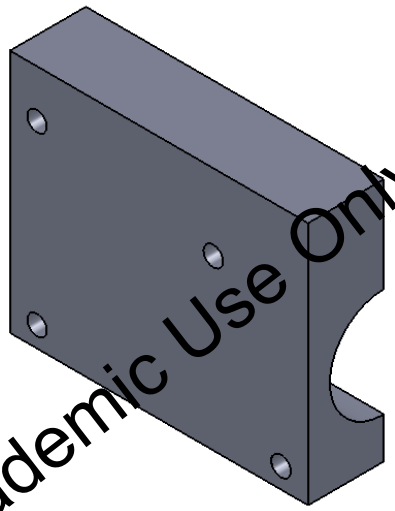

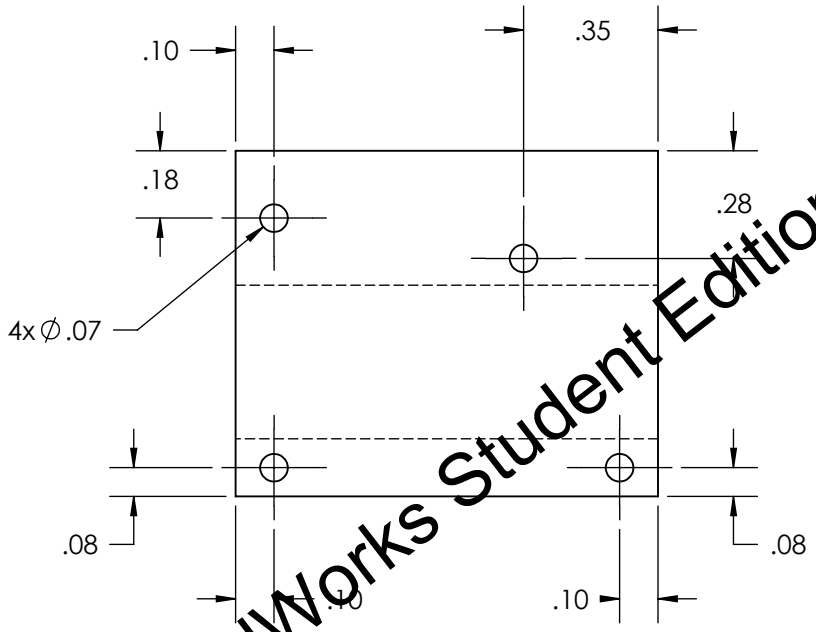

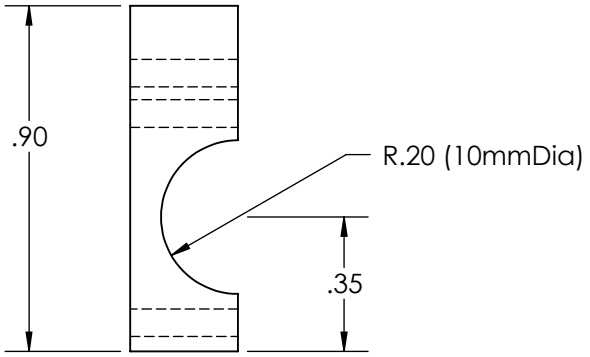

ME430 Winter 2009	TOLERANCE: ±.01	MATERIAL: Delryn
	SCALE: 2:1	DRAWING #: 006
	UNITS: Inches	TITLE: Motor Mount Cover
NEXT ASSY: 007	DATE: 6-3-2010	NAME: Josh Bugni & Andy Sofranko

Mechanical Engineering CAL POLY

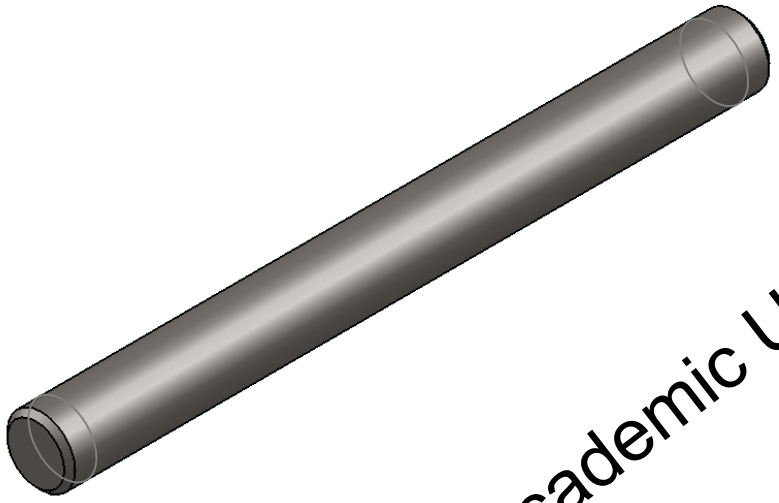

ME430 Winter 2009	TOLERANCE: ±.01	MATERIAL: Steel
	SCALE: 4:1	DRAWING #: 007
	UNITS: Inches	TITLE: Pinion Shaft
NEXT ASSY:008	DATE: 6-3-2010	NAME: Josh Bugni & Andy Sofranko

Mechanical Engineering CAL POLY

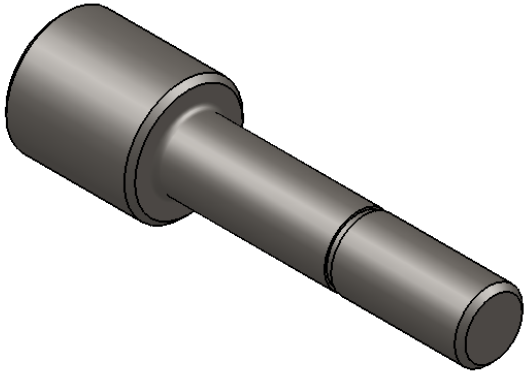

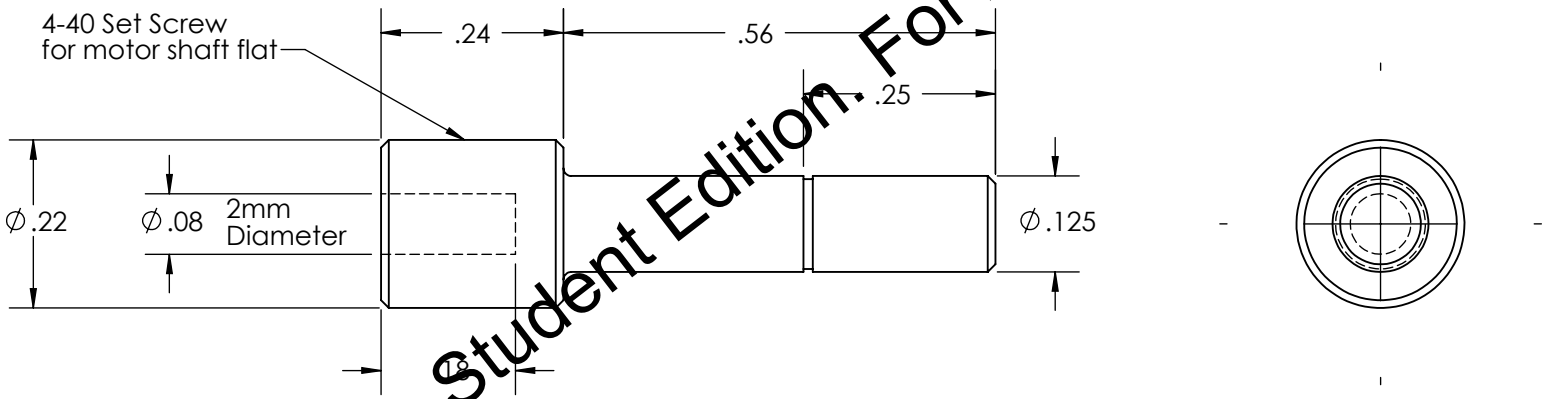

ME430 Winter 2009	TOLERANCE: ±.01	MATERIAL: Steel
	SCALE: 2:1	DRAWING #: 008
	UNITS: Inches	TITLE: Motor Adapter Shaft
NEXT ASSY: 009	DATE: 6-3-2010	NAME: Josh Bugni & Andy Sofranko

Mechanical Engineering
CAL POLY

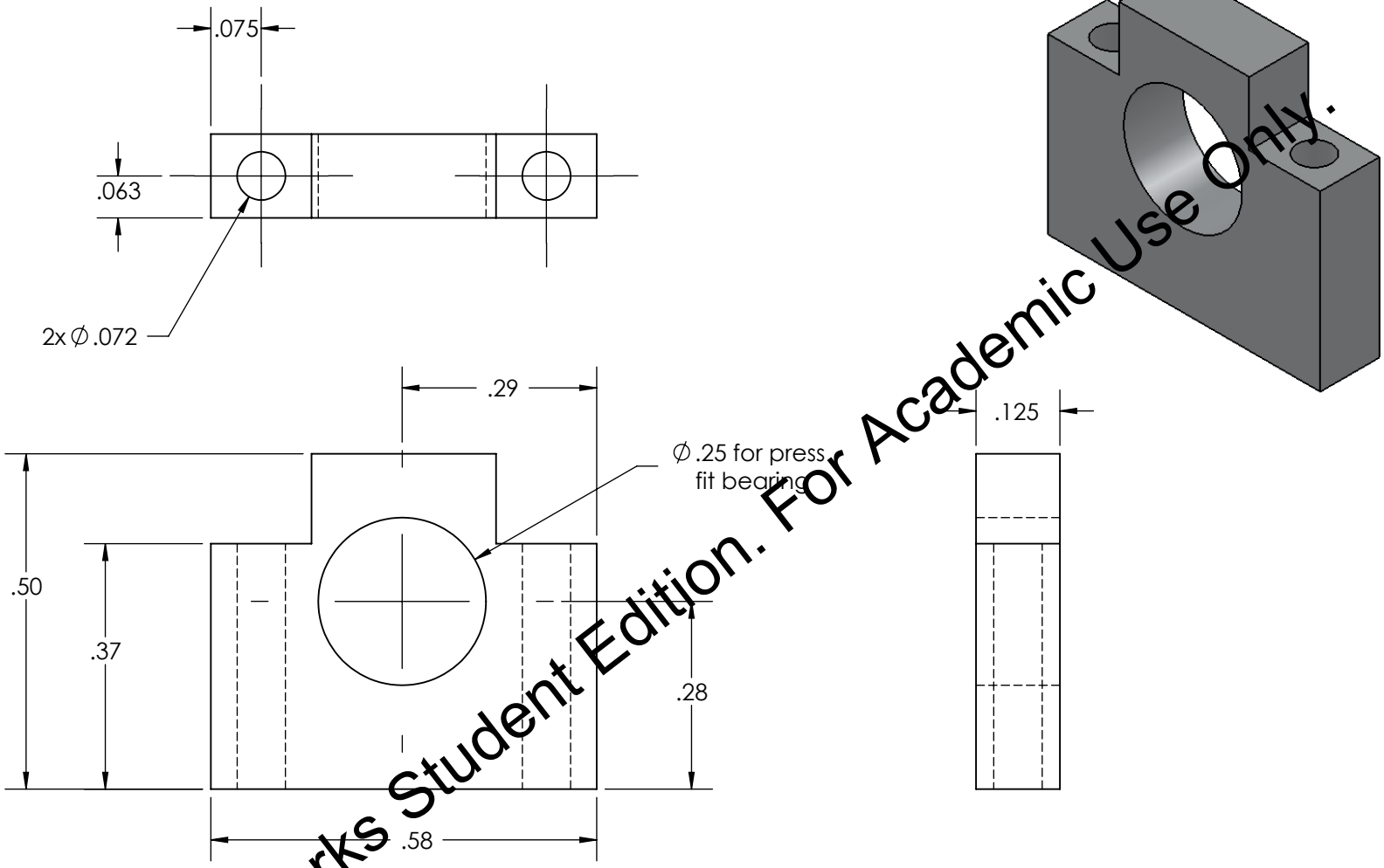

ME430 Winter 2009	TOLERANCE: ±.01	MATERIAL: Alluminum
	SCALE: 2:1	DRAWING #: 009
	UNITS: Inches	TITLE: Pillow Block
NEXT ASSY: 010	DATE: 6-3-2010	NAME: Josh Bugni & Andy Sofranko

Mechanical Engineering
CAL POLY

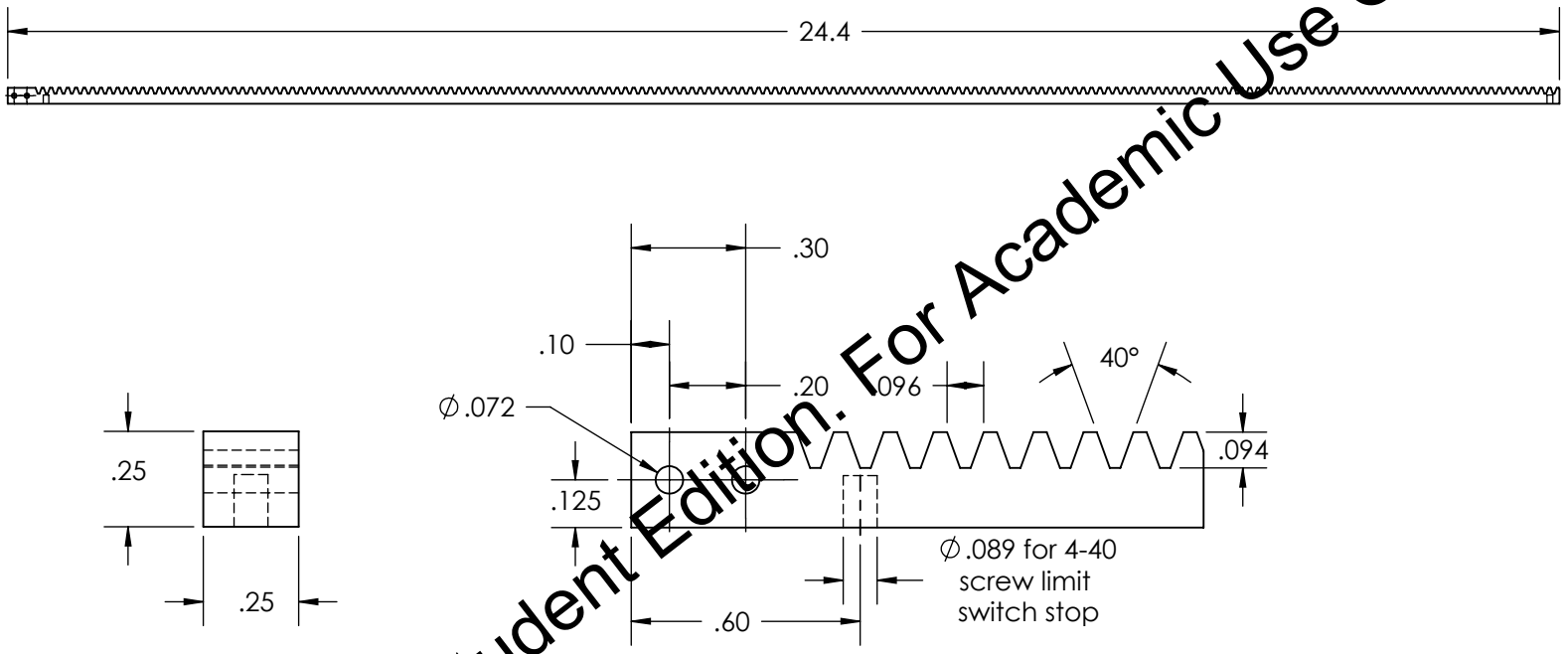

ME430 Winter 2009	TOLERANCE: ±.01	MATERIAL: Aluminum
	SCALE: 2:1	DRAWING #: 010
	UNITS: Inches	TITLE: Rack
NEXT ASSY: 011	DATE: 6-3-2010	NAME: Josh Bugni & Andy Sofranko

Mechanical Engineering CAL POLY

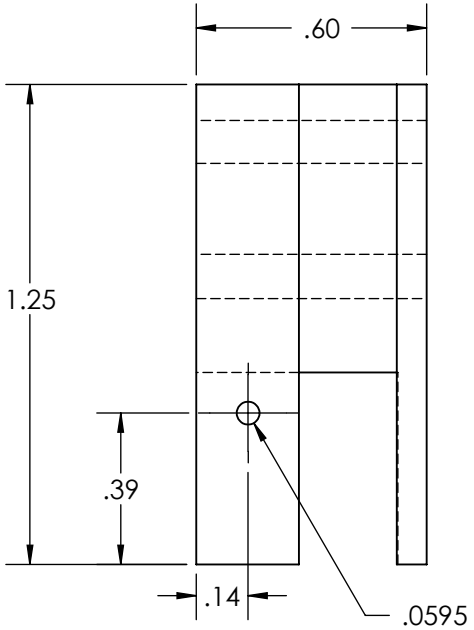

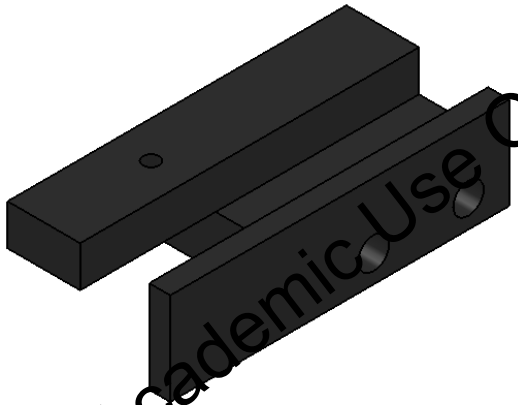

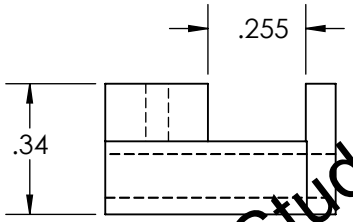

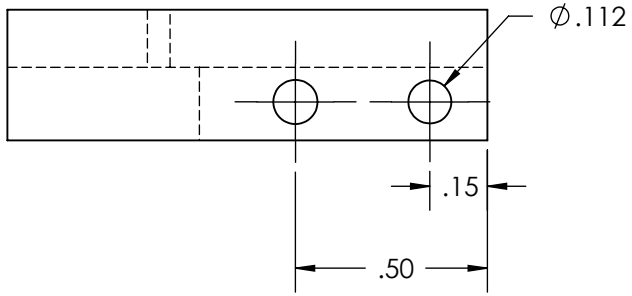

ME430 Winter 2009	TOLERANCE: ±.01	MATERIAL: Delryn
	SCALE: 2:1	DRAWING #: 011
	UNITS: Inches	TITLE: Rear Sleeve
NEXT ASSY: 012	DATE: 6-3-2010	NAME: Josh Bugni & Andy Sofranko

Mechanical Engineering
CAL POLY

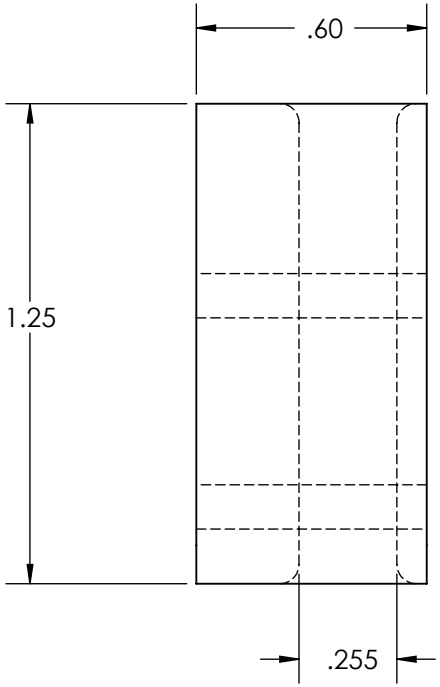

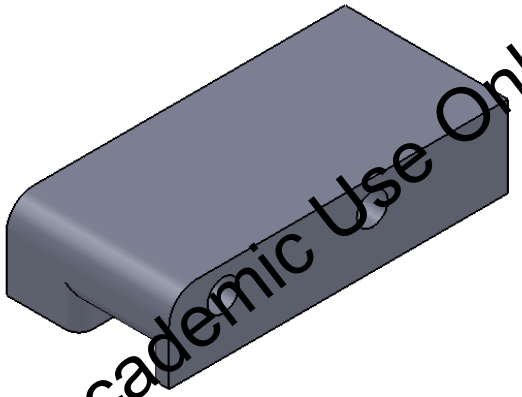

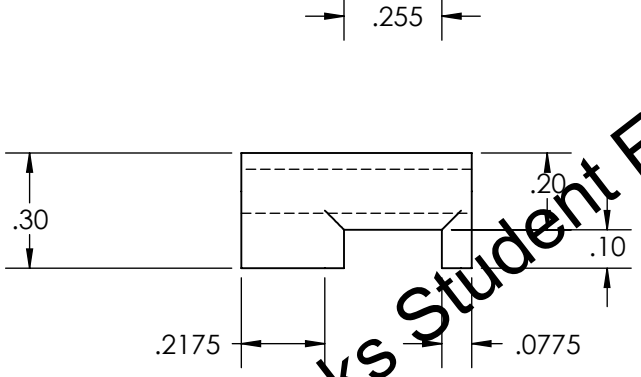

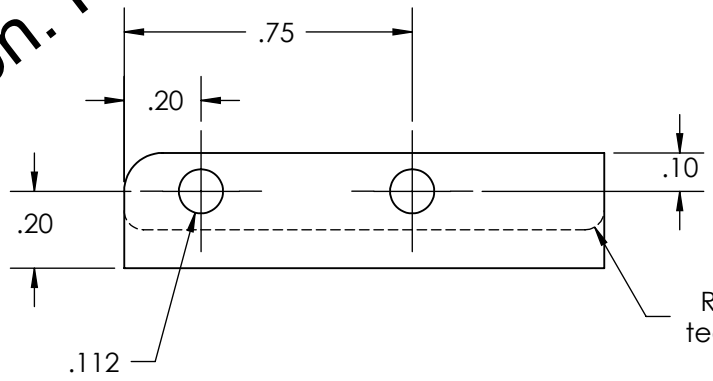

ME429 Winter 2009	TOLERANCE: ±.01	MATERIAL: Delryn
LEC SEC:	SCALE: 2:1	DRAWING #: 013
LAB SEC:	UNITS: Inches	TITLE: Rear Top Sleeve
NEXT ASSY: 014	DATE: 1-7-2010	NAME: Josh Bugni & Andy Sofranko

Mechanical Engineering
CAL POLY

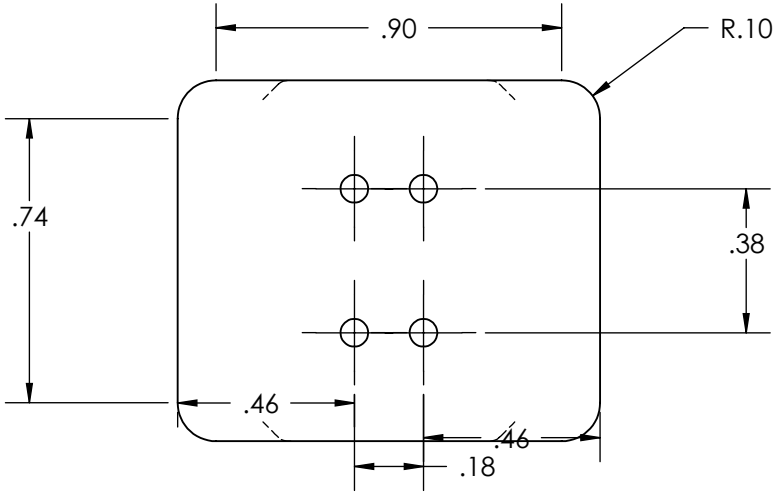

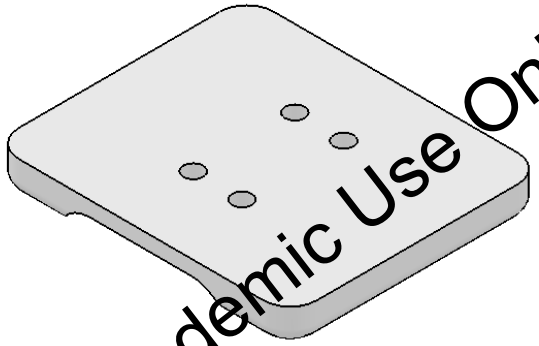

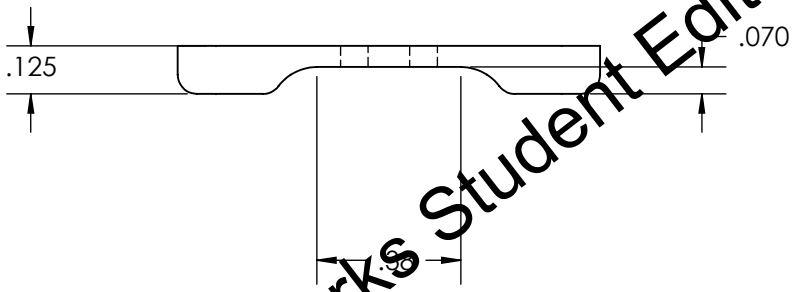

ME430 Winter 2009	TOLERANCE: ±.01	MATERIAL: Teflon
	SCALE: 4:1	DRAWING #: 014
	UNITS: Inches	TITLE: Foot
NEXT ASSY: 015	DATE: 6-4-2010	NAME: Josh Bugni & Andy Sofranko

Mechanical Engineering CAL POLY

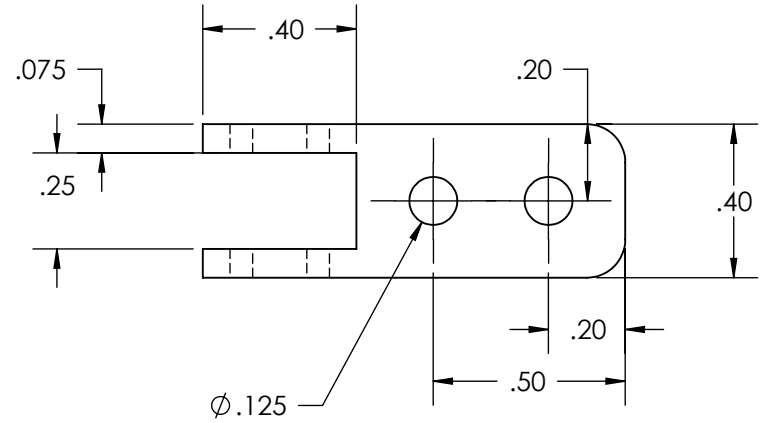

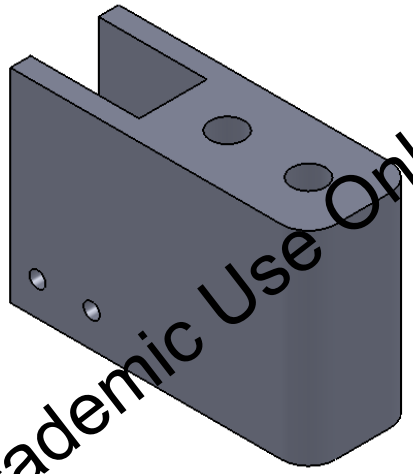

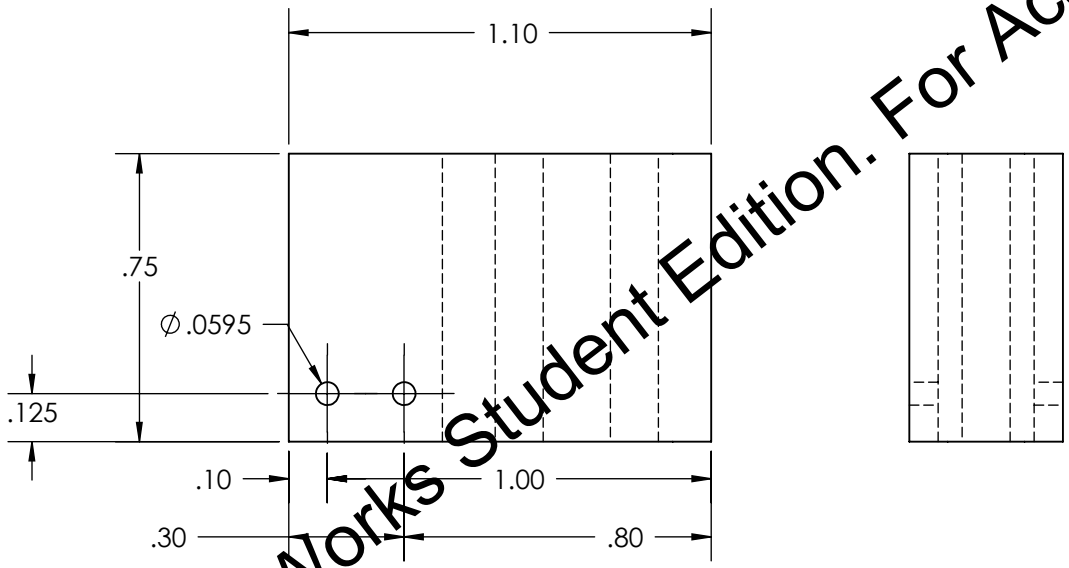

ME430 Winter 2009	TOLERANCE: ±.01	MATERIAL: Delryn
	SCALE: 2:1	DRAWING #: 015
	UNITS: Inches	TITLE: Rack Tip
NEXT ASSY: 016	DATE: 6-4-2010	NAME: Josh Bugni & Andy Sofranko

Mechanical Engineering
CAL POLY

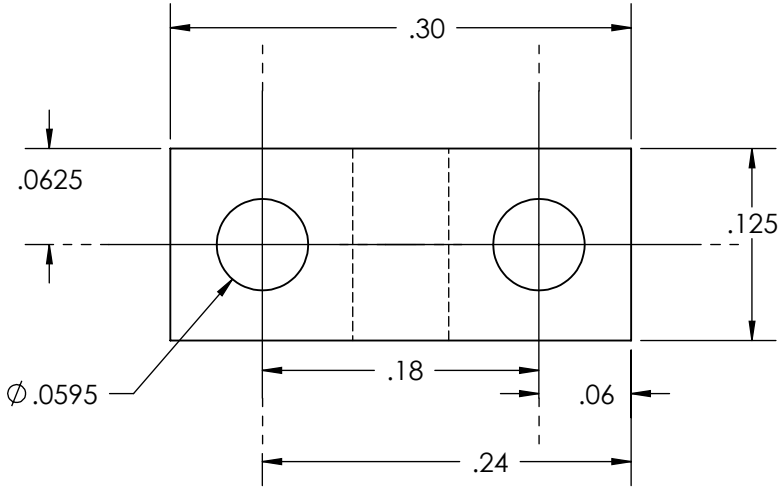

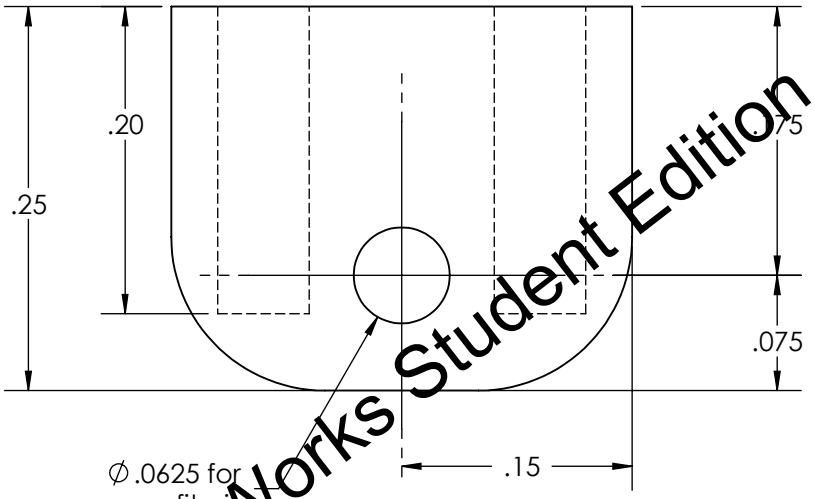

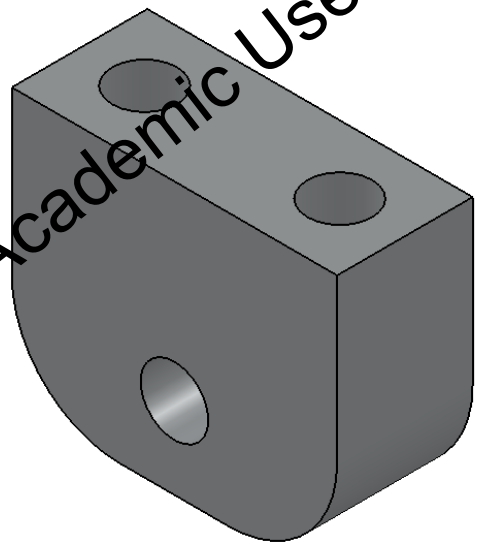

ME429 Winter 2009	TOLERANCE: ±.01	MATERIAL: Alluminum
	SCALE: 4:1	DRAWING #: 016
	UNITS: Inches	TITLE: Hinge on Foot Base
NEXT ASSY: 017	DATE: 6-4-2010	NAME: Josh Bugni & Andy Sofranko

Mechanical Engineering
CAL POLY

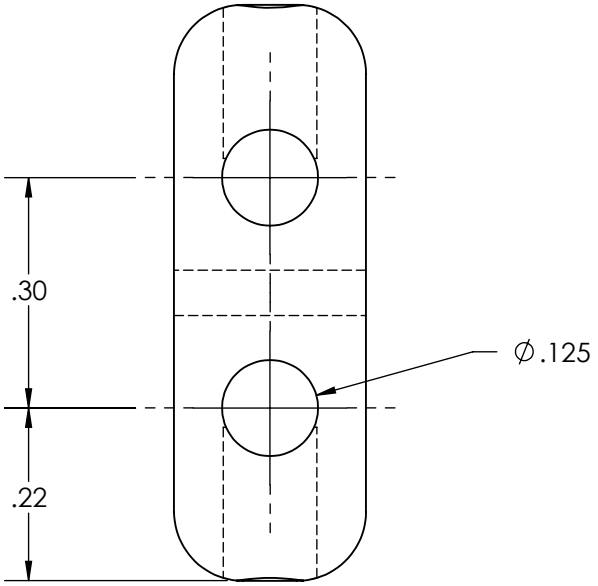

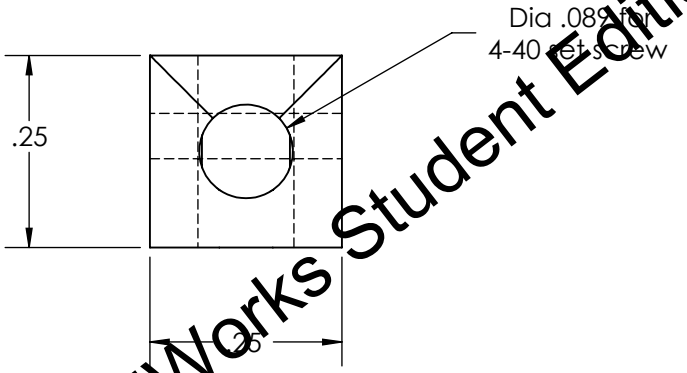

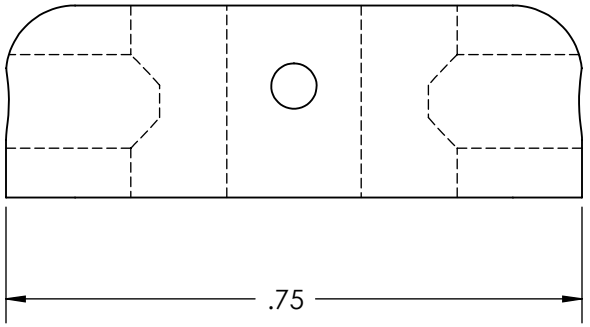

ME430 Winter 2009	TOLERANCE: ±.01	MATERIAL: Aluminum
	SCALE: 4:1	DRAWING #: 017
	UNITS: Inches	TITLE: Rocker
NEXT ASSY: 018	DATE: 6-3-2010	NAME: Josh Bugni & Andy Sofranko

Mechanical Engineering
CAL POLY

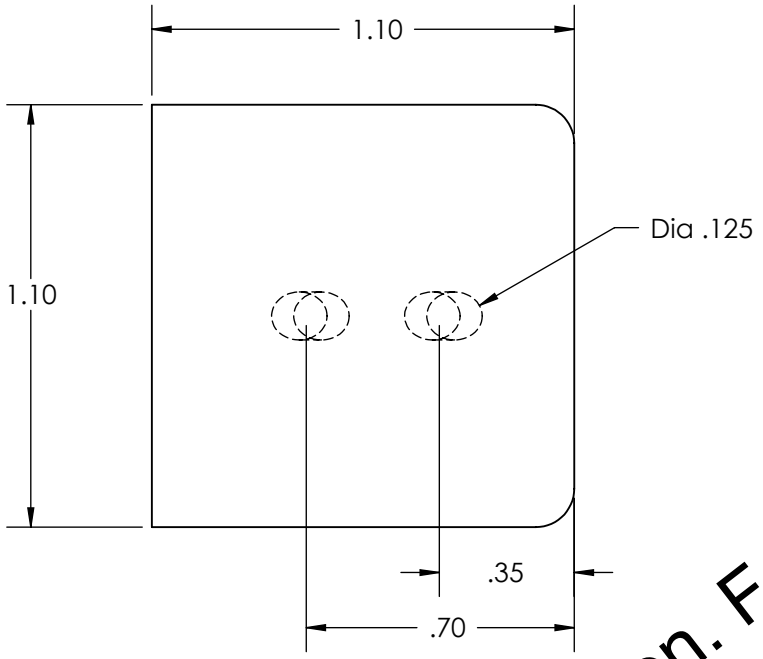

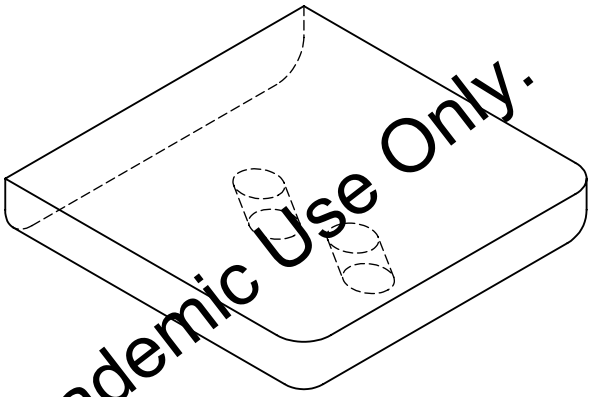

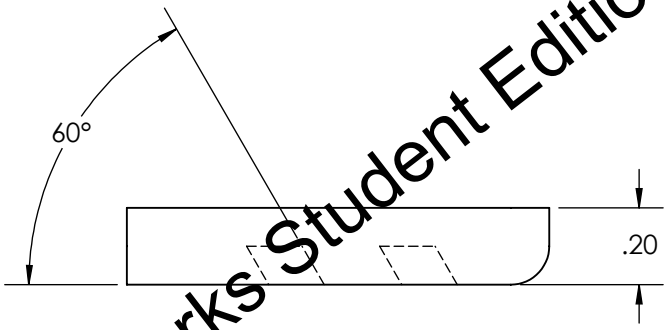

ME430 Winter 2009	TOLERANCE: ±.1	MATERIAL: Delryn
LEC SEC:	SCALE: 2:1	DRAWING #: 018
LAB SEC:	UNITS: Inches	TITLE: Fin
NEXT ASSY: 019	DATE: 1-7-2010	NAME: Josh Bugni & Andy Sofranko

Mechanical Engineering
CAL POLY

Table H.1- Parts List and Price

Mcmaster Carr							
Name	Part Number	Price	Amount	Price Total	Percent of Part Used	Price per unit used	Notes
retaining rings	97633A110	$4.57	1	$4.57	0.03	$0.14	Pack of 100
Base - Bar Stock	8975K311	$20.37	1	$20.37	0.10	$2.11	1.5 x 2 x 12 inches
Rack	86895K42	$15.10	1	$15.10	0.36	$5.44	.25 in x .25 in x 6 feet
4-40 set crew	90251A108	$8.19	1	$8.19	0.12	$0.98	Pack of 25
1--64	91773A170	$13.41	1	$13.41	0.14	$1.88	Pack of 100
4-40 sleeve mount screws	91773A115	$5.83	1	$5.83	0.16	$0.93	Pack of 100
Dowel Pins	98381A415	$11.65	1	$11.65	0.02	$0.23	100 per package
Sleeve Bearing	6381K405	$3.56	3	$10.68	1.00	$10.68	neg 350 deg c
Delrin	8578K414	$67.20	1	$67.20	0.12	$7.90	6 x 6 x .5 inches
Teflon	1019T12	$19.64	1	$19.64	0.03	$0.55	6in x 6in
motor adapter shaft 5 inch	1263K165	$4.11	1	$4.11	0.16	$0.66	7/32 shaft x 5in long
Pinion Shaft	1327K933	$3.56	1	$3.56	0.46	$1.64	1/8 in Shaft x 3 in long
Foot Assembly Shaft	1327K97	$4.81	1	$4.81	0.63	$3.01	8 inches
Grease For Gears - Shell Alvania EP	1431K1	$9.79	1	$9.79	0.01	$0.10	neg 35 deg c
Berg Gears							
	Part Number	Price	Amount	Price Total			
Helical Gear 40 Tooth	H64A10-40	$30.51	1	30.51	1.00	$30.51	Pitch of 64, Bore of 1/8 in
Helical Gear 20 Tooth		$23.13	1	23.13	1.00	$23.13	
Pinion Gear	PX24S-18	$18.17	1	18.17	1.00	$18.17	Pitch of 24, 18 teeth
Other Suppliers							
Limit Switches (Digikey.com)	SW843-ND	$1.82	1	$1.82	1.00	$1.82	Two different part numbers for different lead orientation
	SW842-ND	$1.82	1	$1.82	1.00	$1.82	
20 degree Chamfer Tool (Harvey Tool)	18720-C3	$18.80	1	$18.80	1.00	$18.80	
1024 DC servo motor		$200.00	1	$200.00	1.00	$200.00	Motor and Gear Head estimate from MicroMo
			Raw Parts Total	**$493.16**	Percent Parts Used Total	**$330.48**	

Component Specifications

Pinion
Pitch - 32
Pitch Diameter - .75 inches
Pressure Angle – 20°
Number of Teeth – 18
AGMA Quality – 5
Material – Cold Rolled Steel
Bore - 1/8 inch
Face Width - ¼ inch
Overall width – ½ inch
Outside Diameter 0.833 inches
Part Number – PX24S-18
From Berg Gears

Helical Gears
Pitch - 64
Pitch Diameter - .4419 inches
Pressure Angle – 20°
Number of Teeth – 20 and 40
AGMA Quality – 10
Bore - 1/8 inch
Face Width – 1/8 inch
Overall width – 5/16 inch
Part Number – H64A10-R20
H64A10-R40
From Berg Gears

Retaining Rings
External Snap
For Shaft 1/8 inch Diameter
Fits Groove Diameter - .117 inches
Fits Groove Width - .012 inches
Thickness .01 inches
Material – Steel

Large Screws for Sleeve Mount
4-40
Length – 1 inch
Tap Hole Size - .089 inches
Clearance Hole Size - .112 inches
Screw Head Diameter - 0.211 inches
Screw Head Height – 0.086 inches

Small Screws
1-64
Length – ½ inch
Tap Hole Size - .089 inches
Clearance Hole Size - .072 inches
Screw Head Diameter - 0.137 inches
Screw Head Height – 0.061 inches

Rack Stock Material
Aluminum – 2024-T4
Sy – 42 to 45 Kpsi
Su – 16-68 Kpsi
Hardness - Brn Hardness 120
Temp Rating: -195°C to +184°C

Base Material
Aluminum – 6061 –T3
Hardness - 60-95 Brinell
Temp Rating: -320°F to +300°F (-196°C to +150°C)

Foot Base Material
Teflon
Temp rating – up to 500°F
Hardness - Shore D52

Washers
Nylon
Inside diameter – 1/8 inches
Outside Diameter – 0.2 inches
Thickness – 0.02 to 0.04

Delrin
Material - PTFE-Filled Delrin (Delrin AF)
Temp Rating: 40°F to +185°F (-196°C to +150°C)
Hardness - Rockwell R118-R121

Motor
1024-006S
Diameter - 10 mm
5 volts, .2 Amps
No load Speed – 13200 rpm
Stall Torque – 2.34 mNm

Pins
Material - Hardened Steel
Diameter – 1/6 inch
Length – ¼ inch

Bearings
Material - Alloy 932 (SAE 660) Bronze
Inside Diameter – 1/8 inch
Outside Diameter – ½ inch
Temp Rating: -350°F to +450°F (-212°C to +232°C)

Shafts
Pinion Shaft
Material - 303 Stainless Steel
Pinion Shaft Diameter – 1/8 inch
Motor Adapter Shaft - Diameter – 7/32

Gear Grease
Synthetic Lithium Grease
Temp Rating: -50°F to +400°F (-46°C to +205°C)

Appendix I Works Cited

Beer, Ferdinand Pierre, E. Russell Johnston, and John T. DeWolf. *Mechanics of Materials*. Boston: McGraw-Hill Higher Education, 2006. Print.

Budynas, Richard G., J. Keith. Nisbett, and Joseph Edward. Shigley. *Shigley's Mechanical Engineering Design*. Boston: McGraw-Hill, 2008. Print.

Fox, Robert W., Alan T. McDonald, and Philip J. Pritchard. *Introduction to Fluid Mechanics*. New York: Wiley, 2004. Print.

Incropera, Frank P. *Introduction to Heat Transfer.* Hobokenm NJ: Wiley, 2007. Print.